https://doi.org/10.5194/os-2022-18
Preprint. Discussion started: 11 April 2022

Ocean Science
Discussions
Open Access
EGU

Exceptional freshening and cooling in the eastern subpolar North Atlantic caused by reduced Labrador Sea surface heat loss

Alan D. Fox[1], Arne Biastoch[2,3], Stuart A. Cunningham[1], Neil Fraser[1], Patricia Handmann[2], N. Penny Holliday[4], Clare Johnson[1], Torge Martin[2], Marilena Oltmanns[4], Willi Rath[2], Siren Rühs[2,5], Alejandra Sanchez-Franks[4], and Christina Schmidt[2, 6]

[1]Scottish Association for Marine Science, Oban, UK
[2]GEOMAR Helmholtz Centre for Ocean Research Kiel, Kiel, Germany
[3]Kiel University, Kiel, Germany
[4]National Oceanography Centre, Southampton, UK
[5]now at: Institute for Marine and Atmospheric research Utrecht, Utrecht University, Netherlands
[6]now at: Climate Change Research Centre and the Australian Centre for Excellence in Antarctic Science, University of New South Wales, Sydney, NSW, Australia
*Corresponding author: alan.fox@sams.ac.uk

Correspondence: Alan D. Fox (alan.fox@sams.ac.uk)

Abstract. Observations of the eastern subpolar North Atlantic in the 2010s show exceptional freshening and cooling of the upper ocean, peaking in 2016 with the lowest salinities recorded for 120 years. Published theories for the mechanisms driving the freshening include: reduced transport of saltier, warmer surface waters northwards from the subtropics associated with reduced meridional overturning; shifts in the pathways of fresher, cooler surface water from the Labrador Sea driven by changing patterns of wind stress; and the eastward expansion of the subpolar gyre. Using output from a high-resolution hindcast model simulation, we propose that the primary cause of the exceptional freshening and cooling is *reduced surface heat loss in the Labrador Sea*. Tracking virtual fluid particles in the model backwards from the eastern subpolar North Atlantic between 1990 and 2020 shows the major cause of the freshening and cooling to be an increased outflow of relatively fresh and cold surface waters from the Labrador Sea; with a minor contribution from reduced transport of warmer, saltier surface water northward from the subtropics. The cooling, but not the freshening, produced by changing proportions of source waters is mitigated by reduced along-track heat loss to the atmosphere in the North Atlantic Current. We analyse modelled boundary exchanges and water mass transformation in the Labrador Sea to show that since 2000, while inflows of lighter surface waters remain steady, the increasing output of these waters is due to reduced surface heat loss in the Labrador Sea beginning in the early 2000s. Tracking particles further upstream reveals the primary source of the increased volume of lighter water transported out of the Labrador Sea is increased recirculation of water, and therefore longer residence times, in the upper 500–1000 m of the subpolar gyre.

https://doi.org/10.5194/os-2022-18
Preprint. Discussion started: 11 April 2022

1 Introduction

Climate models, supported by observations, consistently predict an anomaly in the surface warming over the eastern subpolar North Atlantic driven by ocean circulation – the "warming hole" (IPCC, 2021). Upper ocean temperature and salinity and their variability in this region are governed by the convergence and divergence of heat and salt in the eastern subpolar North Atlantic (Keil et al., 2020). The convergence and divergence are associated with the strength of the Atlantic meridional overturning circulation (AMOC) bringing subtropical-origin water northwards (Robson et al., 2016; Foukal and Lozier, 2018; Bryden et al., 2020); shoaling isotherms and isohalines bringing colder fresher water closer to the surface (Josey et al., 2018); and eastward expansion and contraction of the subpolar gyre (SPG) (Bersch, 2002; Hátún et al., 2005; Bersch et al., 2007; Sarafanov, 2009; Koul et al., 2020), with the accompanying movement of subpolar fronts and changes in the North Atlantic Current (NAC) pathways. The ocean circulation variability is in turn associated with local and remote changes in atmospheric forcing including surface heat fluxes (Josey et al., 2018), shortwave cloud feedbacks (Keil et al., 2020), the leading modes of atmospheric variability in the North Atlantic (Häkkinen et al., 2011; Koul et al., 2020), and wind stress curl patterns (Häkkinen et al., 2011; Chafik et al., 2019; Holliday et al., 2020); as well as upstream freshwater input (Peterson et al., 2006) and internal ocean modes (Johnson et al., 2019).

Within the context of the "warming hole", multiple observations show exceptional freshening and cooling of the upper 500–1000 m of the eastern subpolar gyre (Josey et al., 2018; Holliday et al., 2020) starting around 2012 and running to the end of the 2010s (Figs. 1 and 2). At its peak, around 2016, this represents the strongest freshening event for 120 years (Holliday et al., 2020). Model and observation based analyses have shown decadal variability in heat and salt content to be primarily driven by variability in northward transport of warm, salty waters from the subtropics (Burkholder and Lozier, 2014; Desbruyères et al., 2015; Robson et al., 2016; Foukal and Lozier, 2018; Desbruyères et al., 2021). This provides decadal-scale preconditioning of the upper ocean by reduced AMOC which, when coupled with intense local winter mixing events bringing colder fresher water to the surface (Josey et al., 2018; Bryden et al., 2020), could produce sufficient cooling and freshening to explain the observed recent exceptional event. Alternatively, increased volumes of cold fresh water from the Labrador Current due to changing pathways of this flow driven by winter wind stress, have also been invoked to explain the exceptional low upper ocean salinity observed (Holliday et al., 2020). This follows more closely ideas of redistribution of heat and salt within the subpolar North Atlantic (SPNA) and variability in the intensity and extent of the SPG driving variability in the eastern subpolar North Atlantic (Koul et al., 2020; Chafik et al., 2019). More recent observations of years since 2016 reveal a cooling-to-warming transition induced by increasing transport of warm subtropical waters in the NAC (Desbruyères et al., 2021).

Our aims here are to quantify the relative contributions of annual to decadal variability in ocean circulation, upstream water properties, and local atmosphere-ocean fluxes to the recent exceptional freshening and cooling event of 2012 to 2016 in the eastern subpolar North Atlantic. Using the knowledge gained, we then look at possible mechanisms driving the changes. We use outputs from a hindcast with a high-resolution, eddy-rich ocean model (VIKING20X) (Biastoch et al., 2021), which reproduces the timing and spatial scales and patterns of the exceptional freshening. Using Lagrangian model analysis software (OceanParcels) (Lange and Sebille, 2017; Delandmeter and Van Sebille, 2019), particles, each representing a fixed volume

https://doi.org/10.5194/os-2022-18
Preprint. Discussion started: 11 April 2022

transport, are tracked backwards in time from positions along the upper 500–1000 m of a vertical section spanning the eastern subpolar North Atlantic. The resulting time series of variability in the upstream source volume transports, thermohaline properties, pathways, transit times and along-track property transformation of the modelled water parcels are used to quantify the contributions to the observed freshening and cooling. We couple this Lagrangian analysis with examination of Eulerian model time series and water mass transformation analysis in the model (Walin, 1982; Tziperman, 1986; Speer and Tziperman, 1992; Nurser et al., 1999) to produce a more complete theory of mechanisms driving the exceptional freshening and cooling.

2 Methods

2.1 Hydrodynamic model

We make use of the eddy-rich, nested ocean–sea-ice model configuration VIKING20X (Biastoch et al., 2021), based on the Nucleus for European Modelling of the Ocean code (NEMO, version 3.6) (Madec et al., 2017) and the Louvain la Neuve Ice Model (LIM2) (Fichefet and Maqueda, 1997; Goosse and Fichefet, 1999). In the vertical, VIKING20X uses 46 geopotential z-levels with layer thicknesses from 6 m at the surface gradually increasing to 250 m in the deepest layers. Bottom topography is represented by partially filled cells allowing for an improved representation of the bathymetry and its slopes (Barnier et al., 2006). In the horizontal, VIKING20X has a tripolar grid with 0.25 degree global resolution, which is refined in the Atlantic Ocean to 0.05 degree, yielding an effective grid spacing of 3–4 km in the subpolar North Atlantic. The run used here, VIKING20X-JRA-short, is an experiment forced from 1980 to 2019 by the JRA55-do forcing (version 1.4) (Tsujino et al., 2018), which is branched from a previous hindcast experiment forced by the CORE dataset (version 2) (Griffies et al., 2009; Large and Yeager, 2009) covering the period 1958 to 2009. Three dimensional model output fields are saved as five day means which are used here for the offline Lagrangian particle tracking and water mass transformation analysis. Hindcasts of the past 50–60 years in this eddy-rich configuration realistically simulate the large-scale horizontal circulation, including the AMOC, the distribution of the mesoscale, overflow and convective processes, and the representation of regional current systems in the North and South Atlantic (Biastoch et al., 2021; Rühs et al., 2021).

2.2 Lagrangian particle tracking

Particles are tracked in the VIKING20X model using the Parcels Lagrangian framework v2.2.2 (Lange and Sebille, 2017; Delandmeter and Van Sebille, 2019). About 70,000 particles are released every five days for 30 years, 1990–2019, throughout the top 1000 m along the eastern section of the OSNAP (Overturning in the Subpolar North Atlantic Programme) line, $\mathrm{OSNAP_E}$ (Fig. 3). Each particle is tracked backwards in time for ten years or until it leaves the VIKING20X domain or reaches 20° N. This is a total of 1.5 billion particle-years. The 1990 to 2019 period was chosen to keep the experiment within the post-1980 hindcast period of the VIKING20X-JRA-short simulation and to compare and contrast the early 1990s and late 2010s subpolar gyre index maxima Biastoch et al. (2021).

https://doi.org/10.5194/os-2022-18
Preprint. Discussion started: 11 April 2022

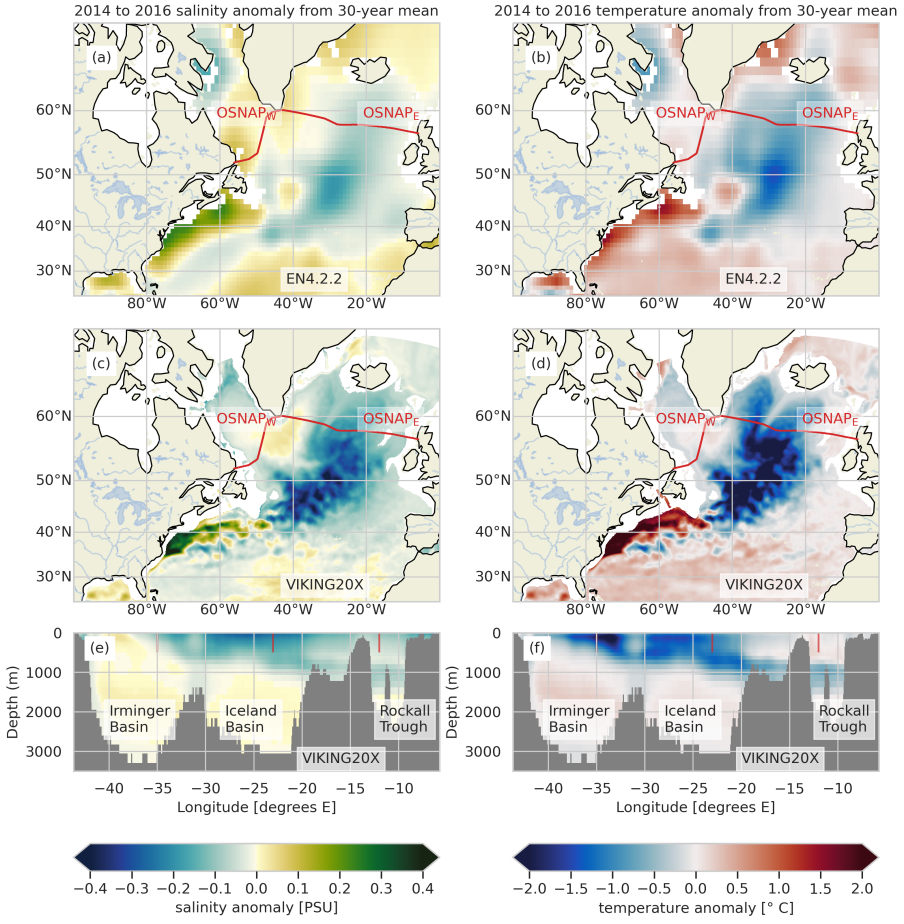

Figure 1. The 2014–16 mean **(a, c)** salinity and **(b, d)** temperature anomalies, relative to the 1990–2019 mean, in the upper 500 m from the **(a, b)** EN4 data set and **(c, d)** VIKING20X model. The OSNAP (Overturning in the Subpolar North Atlantic Programme) observational section (**(e, f)** and red lines in **(a)–(d)**), occupied since 2014 and used here to spawn tracked particles in VIKING20X, traverses the fresh patch in the Iceland and Irminger Basins. In 2014–16 there is a widespread region of fresher than average water in the upper 500 m of the eastern Subpolar Gyre, with a 'compensating' region of raised salinity on the North West Atlantic Continental Shelf and Slope region (NWACSS, 40–50°N, 50–70°W, which includes offshore Slope Sea deep water north of the Gulf Stream). Vertical red lines in **(e,f)** show the position of the time series in Fig. 6.

Particles are advected by the VIKING20X 5-day mean, 3-dimensional velocity fields north of 20° N using a 4th order Runge-Kutta time step scheme with a ten minute time step. No additional diffusion is used. Particle position, velocity, temperature, salinity and model mixed layer depth are recorded every five days along-track.

The initial 2-dimensional, $x-z$, spatial particle distribution along the OSNAP$_E$ section is random, weighted by the magnitude of model velocity normal to OSNAP$_E$ at release time. Each particle therefore represents the same magnitude volume transport normal to OSNAP$_E$, here 0.001797 Sv, with positive transport northward and negative southward. Particles are assumed to

https://doi.org/10.5194/os-2022-18
Preprint. Discussion started: 11 April 2022

Ocean Science
Discussions
Open Access
EGU

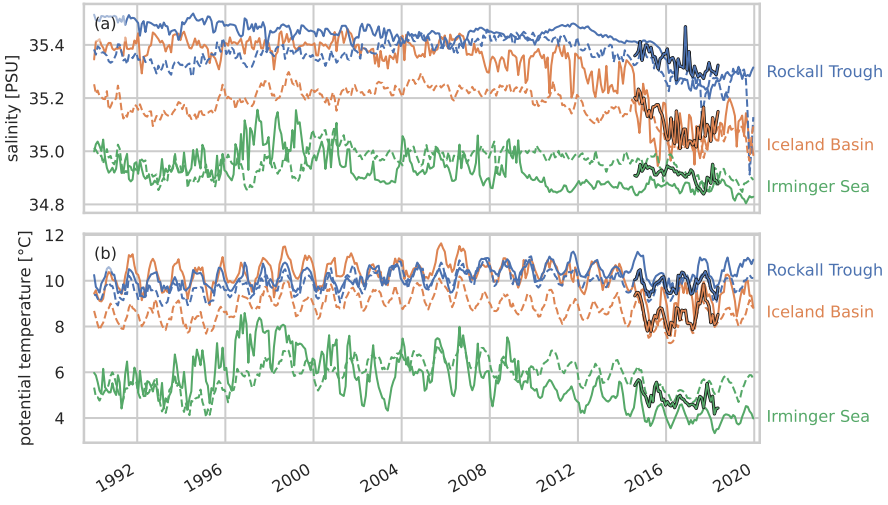

Figure 2. Model (plain solid lines) and observational (EN4, dashed lines; OSNAP, bold lines from 2014) time series of **(a)** salinity and **(b)** temperature at three locations along the eastern section of the OSNAP (Overturning in the Subpolar North Atlantic Programme) line, $\mathrm{OSNAP_E}$ (see Fig. 1 for positions). All time series are monthly means and averaged over the upper 500 m.

maintain these along-track transport values throughout the track, as for streamtubes in steady flow (van Sebille et al., 2018). This assumption is only formally valid when using analytical advection methods for steady flows, but it was shown that the numerical advection method in Parcels can be used for volume transport estimations (Schmidt et al., 2021). We estimate errors by randomly dividing the tracked particles into 32 subsets and calculating the variance among these subsets. These errors are included as error bars. This gives us an estimate of the random errors associated with particle sampling strategy and the effect of unsteady flow on the streamtube assumption. Particle release numbers were set high enough to keep sampling errors small compared to the variability being investigated as is the current standard in following water masses using Lagrangian tools (Schmidt et al., 2021). Systematic biases present in all 32 subsets and associated with either the model flow fields or the streamtube assumption will not be quantified by this method.

Particle upstream origins – Gulf Stream and Labrador Sea – were defined as the region last visited before particles arrived at $\mathrm{OSNAP_E}$ (Fig. 3). A small proportion of water (5–10 %, 2–3 Sv) has an undetermined origin even after 10 years tracking. These 'other' origin particles remained circulating within the eastern subpolar gyre for the full ten years of tracking (apart from a very few which came from the Mediterranean Sea). The paths of Labrador Sea origin tracks were additionally classified by whether they passed through the western Slope Sea region between the Gulf Stream and the shelf slope (which we define as west of 60° W, see New et al. (2021)) – 'loop' path – or took a more direct route – 'direct' path – between leaving the Labrador Sea and arriving at $\mathrm{OSNAP_E}$. We further subdivided Labrador Sea origin tracks by upstream origin (Fig. 3f–i): 'Hudson Bay' describes particles which have entered the Labrador Sea from Hudson Bay; 'Davis Strait' describes particles which entered the Labrador Sea southward through the Davis Strait; 'Greenland Sea' describes particles which have crossed the Greenland-

https://doi.org/10.5194/os-2022-18
Preprint. Discussion started: 11 April 2022

Ocean Science
Discussions
Open Access
EGU

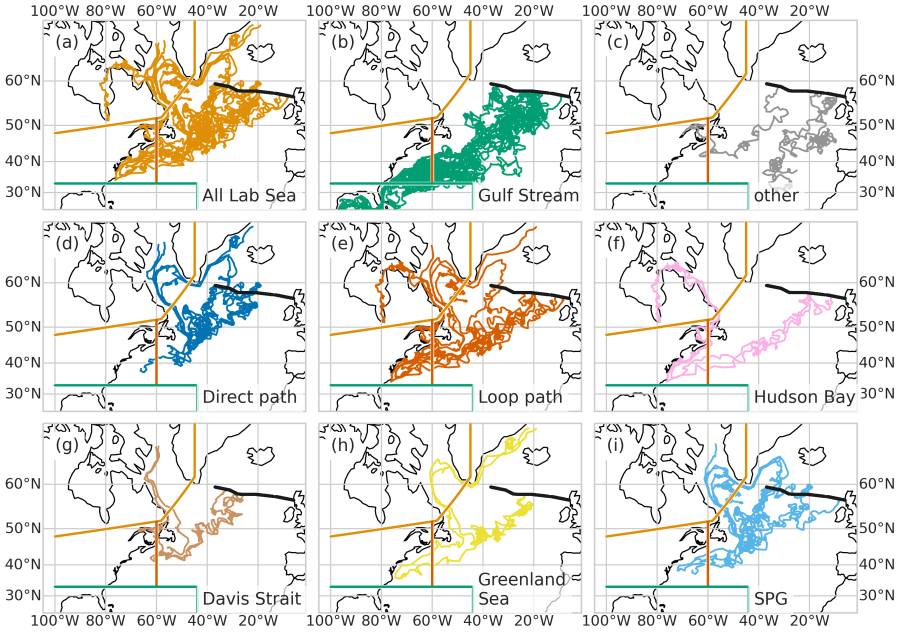

Figure 3. Example particle paths showing the subsets used for identifying sources and pathways. The black line is the section of $OSNAP_E$ where particles are released for backward tracking. The coloured straight lines delimit the sources and pathways: orange – Labrador Sea, green – Gulf Stream, and dark orange – the 'loop' pathway. **(a, b, c)** show the main source subsets: **(a)** Tracks from the Labrador Sea, **(b)** from the Gulf Stream, **(c)** no source determined – 'other' source. **(d, e)** show further refined subsets of **(a)**, highlighting different pathways from the Labrador Sea to $OSNAP_E$: **(d)** the 'direct' path, **(e)** the 'loop' path. **(f)–(i)** show an alternative subset of **(a)**, separating particle tracks according to their source regions further upstream of Labrador Sea: **(f)** Hudson Bay, **(g)** Davis Strait, **(h)** Greenland Sea and **(i)** particles recirculating in the Subpolar Gyre. Occasional particles which appear to originate in the wrong regions, e.g. in panels **(d)** and **(i)**, have completed more than one complete circuit of the SPG in ten years, the path and upstream source are determined on the first circuit.

Scotland ridge southward, mostly through the Denmark Strait from the Greenland Sea, before travelling round the Labrador Sea; and 'SPG' describes particles with Labrador Sea origin which have remained within the SPG for a complete circuit.

In the analysis we exclude any particles which pass north of $OSNAP_E$ between leaving their region of origin and arriving at $OSNAP_E$. This is a common technique in quantitative Lagrangian analysis (van Sebille et al., 2018). The alternative, tracking all particles, counter-intuitively involves tracking particles with negative volume transports and accounting for this in the analysis. This choice makes very little difference to the results, for an ocean in steady state the two approaches would be identical.

Here, we present analyses based on a subset of these particles which cross $OSNAP_E$ in the surface 500 m and east of 37° W (Fig. 3) to focus on the area of maximal cooling and freshening. The western extreme was set at 37° W to sample the northward upper ocean flow in the eastern SPG while not sampling the southward flow east of Greenland. We refer to this section as $OSNAP_{E\text{-}37W\text{-}500m}$. Other subsets of particles crossing $OSNAP_E$ were tried – top 1000 m, upper limb of AMOC

https://doi.org/10.5194/os-2022-18
Preprint. Discussion started: 11 April 2022

($\sigma_0 < 27.62\,\mathrm{kg\,m^{-3}}$), or Iceland Basin only. The results from these alternative subsets (not shown) are qualitatively the same as the results we present here.

Time series are primarily presented plotted against the time the particles cross $\mathrm{OSNAP_E}$. It is also useful to present some time series plotted against the time the particles left the major regions of origin. By grouping particles by their origin-leaving time, using the same 5-day intervals as for the particle releases, we obtain the 5-day mean transport out of the regions of origin of water, which subsequently crosses $\mathrm{OSNAP_{E\text{-}37W\text{-}500m}}$. With a ten year tracking duration, these transports at origin will only be fully 'saturated' between 1990 and 2009, outside this window particle numbers drop off due to the transit times from $\mathrm{OSNAP_E}$. To extend this window we use the fractional distribution, $g(t)$, and cumulative distribution, $h(t) = \int_0^t g(t')dt'$ (where $0 < t < 10\,\mathrm{years}$ and $0 < g(t), h(t) < 1$) of transit times to construct a time-dependent normalization factor, $f(d)$, where d is the date in decimal years:

$$f(d) = \begin{cases} 1 - h(1990 - d) & \text{if } 1980 \leq d < 1990, \\ 1 & \text{if } 1990 \leq d < 2010, \\ 1 - h(d - 2010) & \text{if } 2010 \leq d < 2020. \end{cases} \tag{1}$$

Particle numbers leaving a source at any time are normalized by dividing by this factor. We cut off the extremes where fewer than 60 % of the transports would be sampled, giving a window between mid-1987 and mid-2017 (Fig. 4c).

Average Temperature and salinity (TS) properties are variously calculated as particles cross $\mathrm{OSNAP_E}$, or by averaging T and S from the time each particle leaves the source regions. These averages are performed for the combined sources and for separate sources and pathways. These are all volume-averages of TS over the volume transported.

2.3 Water mass analysis

The rate of formation of a water mass between two isopycnals $M(\rho)$ in some domain can be expressed as

$$M(\rho) = -\frac{\partial F}{\partial \rho} + \frac{\partial^2 D_{diff}}{\partial \rho^2}, \tag{2}$$

where F represents the the transformation driven by surface fluxes along the surface outcrop of the ρ isopycnal (Speer and Tziperman, 1992), and D_{diff} represents the total diapycnal diffusive density flux across the ρ isopycnal resulting from interior mixing (Walin, 1982; Speer and Tziperman, 1992; Nurser et al., 1999; Fox and Haines, 2003). Here F is given by

$$F = \lim_{\Delta\rho \to 0} \frac{1}{\Delta\rho} \int_{outcrop} \mathcal{D}_{in}\, dA, \tag{3}$$

where $\mathcal{D}_{in}$ is the density influx per unit area and A is the surface area outcrop between isopycnals ρ and $\rho + \Delta\rho$. The transformation driven by surface fluxes is divided into heat (F_H) and freshwater fluxes (F_F) (Tziperman, 1986)

$$F = F_H + F_F, \tag{4}$$

https://doi.org/10.5194/os-2022-18
Preprint. Discussion started: 11 April 2022

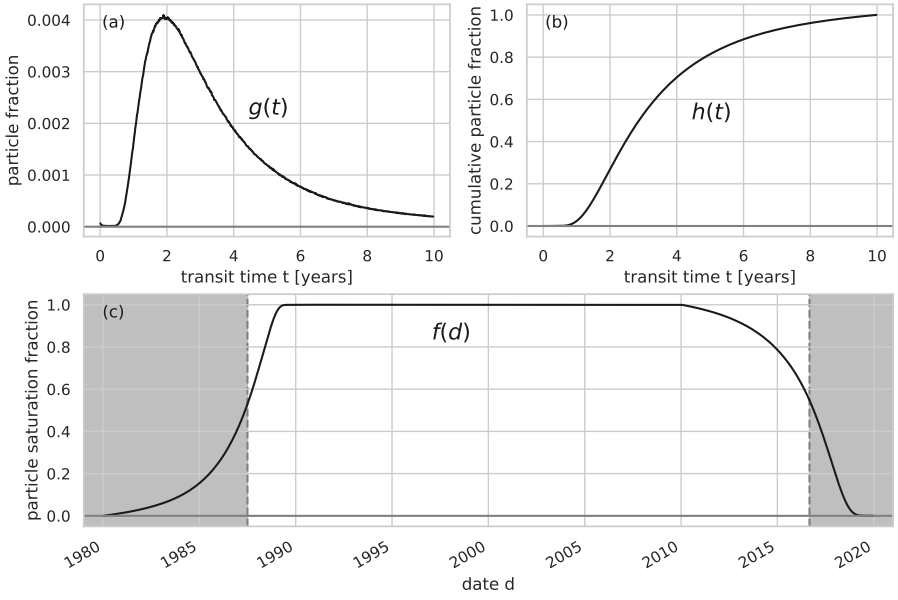

Figure 4. Construction of the factor used to normalize the transports at source and select a window of maximum confidence. **(a)** Histogram of transit times between leaving the source region and crossing OSNAP_E. **(b)** Cumulative histogram showing the fraction of particles transiting in less than each number of days. **(c)** Particle number normalization factor. Numbers of particles leaving source are saturated between 1990 and 2010, outside this range numbers fall off at a rate determined by the transit time. Particle numbers leaving a source at any time are normalized by dividing by this factor. We cut off once fewer than 60% of particles are expected to be recorded (shaded zones).

with

$$F_H = -\lim_{\Delta\rho\to 0}\frac{1}{\Delta\rho}\int_{outcrop}\frac{\rho\alpha\mathcal{H}}{C_p}\,dA, \tag{5a}$$

$$F_F = \lim_{\Delta\rho\to 0}\frac{1}{\Delta\rho}\int_{outcrop}\rho\beta S\mathcal{Q}\,dA + \int_{surface\ \rho'<\rho}\mathcal{Q}\,dA. \tag{5b}$$

where $\mathcal{H}$ is the downward surface heat flux, $\mathcal{Q}$ is the upward freshwater flux, α and β are the thermal expansion and saline contraction coefficients respectively, and C_p is the specific heat capacity.

Integrating Eq. (2) in density, from the lightest ρ_{min} up to ρ, we have the volume transformation budget

$$\underbrace{\frac{\partial V(\rho)}{\partial t}}_{\text{volume tendency}} + \underbrace{\Psi(\rho)}_{\text{outflow}} = -\underbrace{F_H}_{\text{surface heat}} - \underbrace{F_F}_{\text{surface freshwater}} + \underbrace{\frac{\partial D_{diff}}{\partial\rho}}_{\text{diffusive outflux}} \tag{6}$$

where V is the total volume of water with density $< \rho$, and Ψ is the volume flux of water with density $< \rho$ out of the domain.

Volume tendency, outflow and surface influx terms in Eq. (6) can be calculated from the VIKING20X 5-day mean model outputs, the diffusive flux – which we cannot calculate directly from the standard outputs – can then be backed out as the sum of the other four terms.

https://doi.org/10.5194/os-2022-18
Preprint. Discussion started: 11 April 2022

2.4 Observational data

Primarily for model verification, we use ocean observation datasets from EN4 (EN.4.2.2, bias corrections .g10, downloaded 2021-01-12) (Good et al., 2013; Gouretski and Reseghetti, 2010; Gouretski and Cheng, 2020) and OSNAP (Lozier et al., 2019; Li et al., 2021).

2.5 Data analysis software packages

All particle tracking and analysis was done in Jupyter notebooks using Python. The main Python packages used include OceanParcels, Numpy, Scipy, xarray, matplotlib, and cartopy; the full details of all packages and version numbers can be found in the published Jupyter notebooks. All plots use seaborn styles (Waskom, 2021) with all line plots using the 'colorblind' colour palette. Filled contour plots use the cmocean oceanography colormaps (Thyng et al., 2016).

3 The 2012–2016 eastern subpolar North Atlantic freshening event

First we briefly establish the spatial and temporal characteristics of the exceptional freshening and cooling event in the eastern subpolar North Atlantic beginning around 2012 (Figs. 1 and 2) and show that the VIKING20X model captures enough detail to be a useful tool to evaluate the possible causes (for more detailed description of the observations see (Holliday et al., 2020)). Spatial patterns of salinification/freshening and warming/cooling in the observations and model are very similar (Fig. 1a–d shows 2014 to 2016 anomalies from the 1990 to 2019 means). Both the EN4 observations and the VIKING20X model show an extensive area of upper ocean freshening and cooling in the eastern subpolar North Atlantic in 2014 to 2016, with strong warming and salinification in the NWACSS (North West Atlantic Continental Shelf and Slope, 40–50°N, 50–70°W, which includes offshore Slope Sea deep water north of the Gulf Stream) region. There is also warming and salinification in the subtropical gyre (south of 35° N), the southern Labrador Sea and north of the Greenland-Scotland ridge in both model and observations. While these spatial patterns are similar, VIKING20X anomalies are generally about 50 % larger than the observed.

Time series of 500 m depth-mean temperature and salinity at three points along $\mathrm{OSNAP_E}$ (Rockall Trough at 12° W, Iceland Basin at 23° W, and Irminger Sea at 35° W, Fig. 2) from VIKING20X and EN4 show the fastest freshening and cooling at OSNAP latitudes occur in the Iceland Basin through 2014 and 2015, with lowest temperatures and salinities recorded in 2016. During the relatively short OSNAP observational period, 2014 to 2018, the model temperature and salinity signals closely track the OSNAP observational data on annual timescales, though not matching all the higher frequency variability. Compared to EN4, VIKING20X has a large-scale warm, salty bias and a freshening trend of 0.1–0.2 PSU over 30 years in the upper subpolar ocean, particularly in the Iceland Basin and Rockall Trough. If we correct this large-scale bias and trend, a common feature of unconstrained model hindcasts, the model overestimation of 2014 to 2016 anomalies (Fig. 1a–d) is reduced and the freshening seen in EN4 in the early 1990s (Fig. 2a) is also seen in VIKING20X. We do not remove these long term, large-scale trends in the analysis presented in order to maintain dynamically consistent model fields.

https://doi.org/10.5194/os-2022-18
Preprint. Discussion started: 11 April 2022

Vertical sections of model temperature and salinity anomalies (Fig. 1e,f) show the cooling and freshening to be confined to the surface 1000 m east of the central Irminger Sea, the region occupied by generally northward flowing waters of the upper limb of the AMOC. Deeper waters show warming and salinification. This compares well with changes described in OSNAP section observational data (Fig. 6 of Holliday et al., 2018). While the OSNAP time series is short, it spans the period of fastest upper ocean freshening and cooling.

The evidence presented here shows that VIKING20X is reproducing the spatial structure and timing of the exceptional freshening event, while somewhat overestimating the amplitude. As a hindcast, VIKING20X is driven by reanalysis surface forcing but runs freely without data assimilation or relaxation to observations, so the similarity to observations is a product of the external forcing and modelled ocean dynamics. As such, the skill exhibited in reproducing the observations supports the idea that we can use the VIKING20X model to help diagnose the causes of the exceptional freshening event.

There are fundamentally only three possible contributions to the exceptional freshening and cooling observed in the eastern subpolar North Atlantic. Firstly, changing proportions of transport coming from the various upstream sources (including the introduction of new sources). Each different upstream source has different average temperature and salinity (TS) properties, so combining them in changing ratios will change TS properties in the eastern subpolar North Atlantic. Secondly, changing TS properties of transports out of the individual source regions. This could alter TS properties in the eastern subpolar North Atlantic even without any change in relative volume transports. And, finally, local processes – surface fluxes and internal mixing – including processes along-track between the upstream source and the eastern subpolar region, causing changing fluxes of freshwater and heat between the upper eastern subpolar North Atlantic waters and the surrounding waters and the atmosphere.

4 Lagrangian particle tracking results

4.1 Changing volume transports by source and pathway

Annual mean total upper ocean volume transports in VIKING20X across $\text{OSNAP}_{\text{E-37W-500m}}$ (Fig. 5) are high (20 Sv) prior to 1996, reduce by 10–20 % between 2000 and 2009, before returning to 20 Sv after 2016. Isolating these transports by source and pathway shows gradually decreasing volumes of Gulf Stream source waters since 1996. For Labrador Sea source waters the picture is mixed, with the loop path transport declining similarly to the Gulf Stream source transports, while the direct path transports increase rapidly between 2008 and 2016. As a consequence, prior to 1996, water crossing $\text{OSNAP}_{\text{E-37W-500m}}$ had 2.5 times as much Gulf Stream as combined Labrador Sea source water, by 2016 the ratio was 1:1. Notice differences here with the modelling work of Koul et al. (2020) which, also using particle tracking but in a coarser resolution model, find a maximum of 11 % of near-surface water in the eastern subpolar North Atlantic to be of subpolar (Labrador Sea) origin. Here we find never less than 25 %, and up to 45 % of northward transport to be of subpolar origin.

In the 1990s both loop and direct paths from the Labrador Sea paths are equally important with contributions of ∼2.5 Sv each, in the 2010s the Labrador Sea contribution mainly consisted of waters that followed the direct path (∼7.5 Sv), while the loop path contribution becomes small (∼1.0 Sv). A small but fairly constant proportion of water parcels (5–10 %, 2–3 Sv) have

https://doi.org/10.5194/os-2022-18
Preprint. Discussion started: 11 April 2022

Ocean Science
Discussions
Open Access
EGU

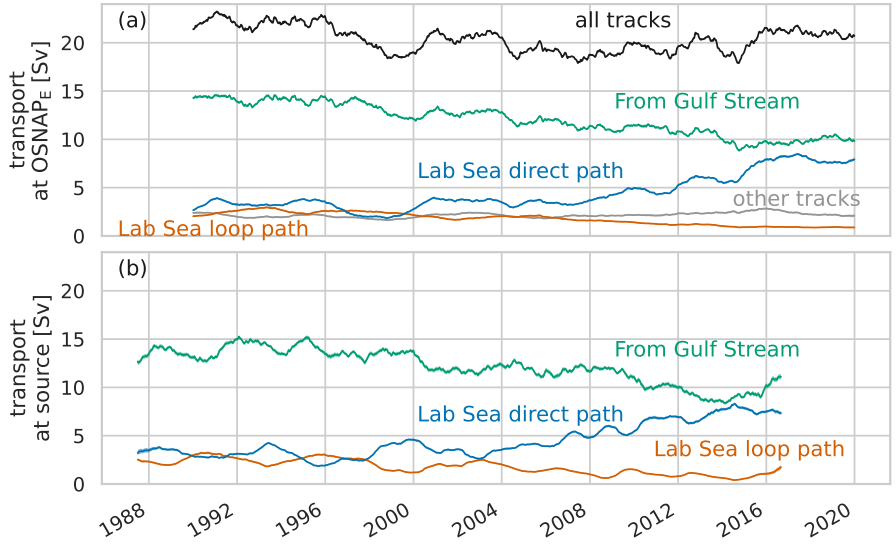

Figure 5. Time series of one-year running mean volume transport across OSNAP$_{E\text{-}37W\text{-}500m}$ by source and pathway plotted against, **(a)**, the time at which water parcels cross OSNAP$_E$ and, **(b)**, the time water parcels leave the source region. The total northward transport (black line) is higher in the 1990s and 2010s and lower in the 2000s. Transport from the Gulf Stream (green) reduces steadily after 1996. From the Labrador Sea, loop path transport (orange) also reduces steadily after 1996 while direct path (blue) increases rapidly after about 2008. Transport with unidentified source after ten years backward tracking is coloured grey. Error bars at ± 1.96 standard deviations around the mean are included but are mostly too narrow to be visible here.

an undetermined source even after ten years tracking. These 'other' source particles (Fig. 3c) remained circulating within the eastern subpolar gyre for the full ten years of tracking (apart from a very few which came from the Mediterranean Sea).

Due to the range of particle travel times (Fig. 4a), plotting volume transports against the time at which particles cross OSNAP$_{E\text{-}37W\text{-}500m}$ temporally smooths changes happening at the sources. This introduces the risk of interpreting rapid changes at the sources as gradual changes OSNAP$_{E\text{-}37W\text{-}500m}$. So we also plot volume transports as particles leave the source region (Fig. 5b) by grouping particles in 5-day bins as they leave the source (see Section 2.2). We can calculate these transports reliably for source-leaving times between mid-1987 and mid-2017, outside this time window we capture a decreasing proportion of the transport. Transports leaving the major sources show similar patterns of variability compared to those at OSNAP, but with source volume transport changes leading OSNAP changes by 3–5 years (corresponding to the most frequent transit times between the source sections and OSNAP, shown in Fig. 4a). In particular transport changes at the sources still appear gradual and maintained over several years, rather than being sudden, step changes. There are signs of an increase in the Gulf Stream and loop path transports leaving the source in 2016, but these increases are yet to be reflected in corresponding increases across OSNAP$_{E\text{-}37W\text{-}500m}$ by the end of 2019.

The general picture over the 30 years of modelled transports across OSNAP$_{E\text{-}37W\text{-}500m}$ is therefore one of gradually reducing volume transports of Gulf Stream origin combined with more rapid increase in total volume transports of Labrador Sea origin

https://doi.org/10.5194/os-2022-18
Preprint. Discussion started: 11 April 2022

after about 2008. This later increase in volume transports of Labrador Sea origin is entirely via the direct path and is new transport rather than a switch in pathways from loop to direct; loop path transports continue slowly declining in parallel with Gulf Stream origin transports. In addition, previously-reported VIKING20X model results Biastoch et al. (2021) show that the denser deep western boundary current (DWBC) transport out of the Labrador Sea decreases after 1996. Together these point to a shift in export volume through the major export routes from the Labrador Sea.

4.2 Temperature and salinity variability, upstream origins and along-track fluxes

Averaged TS properties at the source, of all particles crossing $\text{OSNAP}_{\text{E–37W-500m}}$ at time t, are calculated from the temperature and salinity of each particle as it leaves the source. These are volume averages of the water as it leaves the source. Neither Labrador Sea origin water nor Gulf Stream origin water show freshening or cooling of comparable magnitude to the total freshening and cooling at $\text{OSNAP}_{\text{E-37W-500m}}$ (Fig. 6). In fact, at their Labrador Sea origin, the waters which cross $\text{OSNAP}_{\text{E–37W-500m}}$ between 1998 and 2012 appear to have become warmer and saltier, with only slight source freshening and cooling of waters which cross $\text{OSNAP}_{\text{E–37W-500m}}$ after 2012. Gulf Stream origin water crossing $\text{OSNAP}_{\text{E–37W-500m}}$ after 2012 showed a small amount of freshening and cooling as it left the source, but as for the Labrador Sea origin this signal is small compared to the total overall freshening and cooling at $\text{OSNAP}_{\text{E-37W-500m}}$. There is more variability (and more uncertainty) in 'source' (i.e. 10-years before crossing $\text{OSNAP}_{\text{E-37W-500m}}$) properties of the particles with no identified source (Fig. 6, grey lines). But these form less than 10 % of the overall transport and only show marked source cooling and freshening in particles crossing $\text{OSNAP}_{\text{E-37W-500m}}$ after 2016. So, most of the freshening is not inherent in the individual origins.

From the transports from the different origins and the mean TS properties at each source we can calculate the 'expected' mean properties of water transported across $\text{OSNAP}_{\text{E-37W-500m}}$ in the absence of along-track external fluxes (surface fluxes or mixing with surrounding waters) (dashed black lines in Fig. 6). The difference in properties between these 'expected' values and the recorded properties (solid black lines in Fig. 6) gives the contribution from along-track external fluxes. For salinity these along-track external fluxes act to slightly increase overall mean salinity between source and $\text{OSNAP}_{\text{E-37W-500m}}$. There is a small consistent trend in the magnitude of this contribution, resulting in weaker along-track salinification after about 1998, hence adding to the net freshening during this period. For temperature the along-track external fluxes cool the water, as expected with overall heat loss to the atmosphere in the subpolar North Atlantic. But, in contrast to salinity, the mean along-track external cooling reduces in time from 2.2 °C in 1998 to 1.0 °C in 2017. Note that this reducing trend in along-track externally-driven cooling opposes the observed cooling at $\text{OSNAP}_{\text{E-37W-500m}}$.

4.3 Quantifying the relative contributions to eastern subpolar North Atlantic freshening and cooling

Noting that, by construction, each individual particle transports the same volume, we can write down expressions for the mean temperature and salinity of the volume transported northwards across OSNAP_{E} at time t in terms of the properties and

https://doi.org/10.5194/os-2022-18
Preprint. Discussion started: 11 April 2022

Ocean Science
Discussions
Open Access
EGU

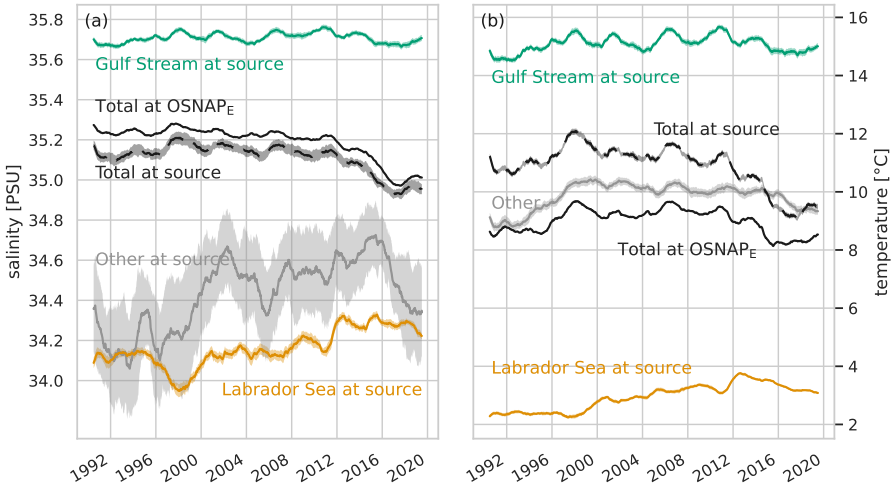

Figure 6. Salinity **(a)** and temperature **(b)** time series at the source and at OSNAP$_E$. For salinity, **(a)**, time series of one-year running mean salinity at OSNAP$_{E\text{-}37W\text{-}500m}$ (solid black lines) and source (dashed black lines) show the mean freshening at the source to be reflected in overall freshening recorded at OSNAP$_{E\text{-}37W\text{-}500m}$. This contrasts with temperatures **(b)** where an overall source cooling (black dashed line) is mitigated by reduced along-track cooling (difference between solid and dashed black lines), resulting in reduced cooling at OSNAP$_{E\text{-}37W\text{-}500m}$ (black solid line). Dividing the properties at source into the three origins, Gulf Stream (green), Labrador Sea (orange), and other (grey), none shows consistent freshening or cooling. The x-axis is the time water parcels cross OSNAP$_{E\text{-}37W\text{-}500m}$. Shaded areas show ± 1.96 standard deviations between the 32 subsets. Uncertainties are larger for the 'other' source because the sample size is smaller and these particles originate in a wide range of conditions throughout the subpolar North Atlantic south of OSNAP$_E$ rather than in tightly defined source regions.

transports from each source and the in-transit change in mean temperature and salinity:

$$\underbrace{\overline{T_o}}_{\text{at OSNAP}_E} = \underbrace{\overline{T_g}\frac{V_g}{V_{all}} + \overline{T_l}\frac{V_l}{V_{all}} + \overline{T_u}\frac{V_u}{V_{all}}}_{\text{at source}} + \underbrace{\overline{\Delta T_t}}_{\text{transit}} \tag{7a}$$

$$\underbrace{\overline{S_o}}_{\text{at OSNAP}_E} = \underbrace{\overline{S_g}\frac{V_g}{V_{all}} + \overline{S_l}\frac{V_l}{V_{all}} + \overline{S_u}\frac{V_u}{V_{all}}}_{\text{at source}} + \underbrace{\overline{\Delta S_t}}_{\text{transit}} \tag{7b}$$

where all variables are functions of the particle release time, t. Here $\overline{T_o}, \overline{S_o}$ represent mean T/S properties at OSNAP$_{E\text{-}37W\text{-}500m}$; V_{all} is the total volume transport across OSNAP$_{E\text{-}37W\text{-}500m}$ at time t; V_g, V_l, V_u represent volume transports from Gulf Stream, Labrador Sea and unidentified 'other' origin respectively (and $V_g + V_l + V_u = V_{all}$); $\overline{T_g}, \overline{S_g}, \overline{T_l}$, *etc.* represent mean properties of particles leaving the relevant origin; and $\overline{\Delta T_t}, \overline{\Delta S_t}$ denote in-transit changes to mean temperature and salinity.

The dependence of V_{all} on V_g, V_l and V_u means we cannot completely separate the contributions to changing temperature and salinity at OSNAP$_E$ from changes to individual properties at, and transports from, the different sources. But we can estimate each of these contributions by varying the six independent variables one at a time, while holding the others at their mean values.

https://doi.org/10.5194/os-2022-18
Preprint. Discussion started: 11 April 2022

Ocean Science
Discussions
Open Access
EGU

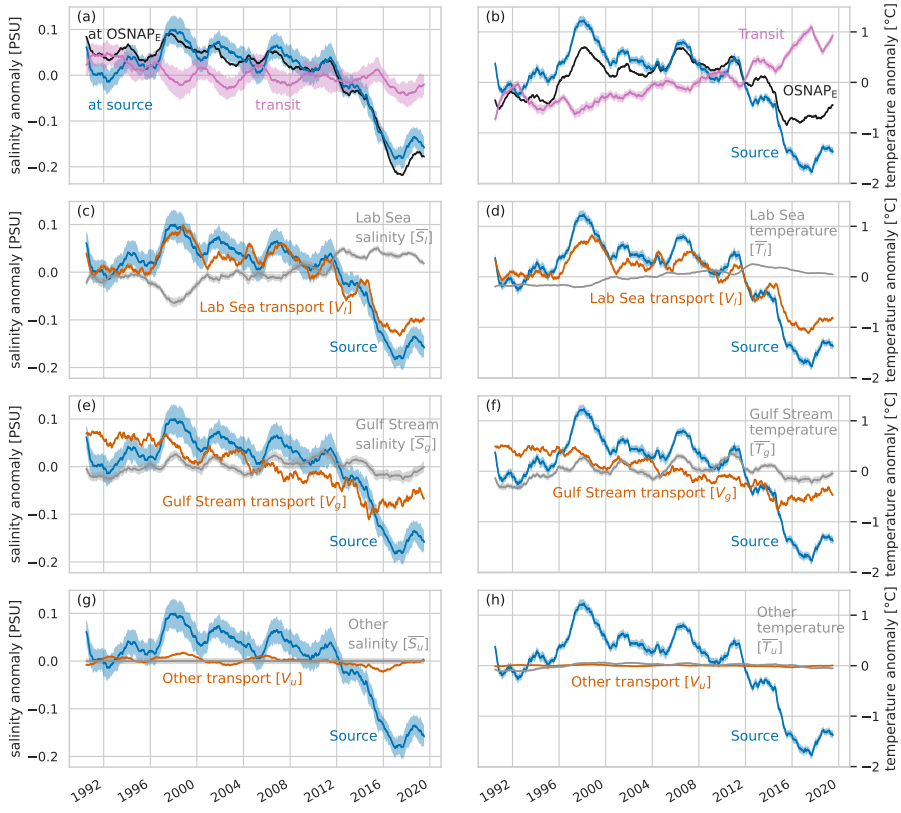

Figure 7. Relative contributions of specific causes to the salinity (left, **(a,c,e,g)**) and temperature (right, **(b,d,f,h)**) changes observed at OSNAP$_{\text{E-37W-500m}}$. These are plots of one-year running mean salinity and temperature anomalies. We see that for salinity, **(a)**, the overall freshening at OSNAP$_{\text{E-37W-500m}}$ (black line) closely follows the freshening of the combined sources (blue line) with a small additional contribution from changes during transit (pink). Temperature, **(b)**, shows in-transit changes (pink) opposing source changes (blue). In the panels below, the contributions of six individual processes (orange and grey lines) to the overall source characteristics (blue lines) are estimated, by holding the other five processes at their mean values (see Eq. 7). These six processes are: volume transport variability (orange lines, V_l, V_g, V_u) and salinity/temperature variability (grey lines, $\overline{S_l}$, $\overline{T_l}$, $\overline{S_g}$, $\overline{T_g}$, $\overline{S_u}$, $\overline{T_u}$) for the Labrador Sea source **(c,d)**, Gulf Stream source **(e,f)**, and other source waters **(g,h)**.

This will tend to underestimate (overestimate) the influence of changes at one source when transports from the other sources are below (above) their mean values.

Following this process (Fig. 7), qualitatively we find that the dominant driver of variability for both salinity and temperature is the volume transported from the Labrador Sea to OSNAP$_{\text{E}}$, V_l. Variability in volume transported from the Gulf Stream V_g plays an additional, but smaller role. Changes in source temperature and salinity show weaker relationships to either overall mean properties at origin or properties at OSNAP$_{\text{E}}$. Only for temperature, we find a notable influence of in-transit, externally driven changes, $\overline{\Delta T_t}$.

https://doi.org/10.5194/os-2022-18
Preprint. Discussion started: 11 April 2022

Table 1. Contributions to the freshening and cooling of water crossing $OSNAP_{E\text{-}37W\text{-}500m}$ in 2016–17 (peak freshening and cooling) relative to 2011–12 (the start of the more rapid freshening and cooling). Contributions are listed by the components described in Section 4.3 and Fig. 7. The largest contribution to both freshening and cooling is made by the changing volume of water of Labrador Sea origin. The single component contributions do not necessarily sum to the total as the component contributions are not independent (see Eq. 7).

Origin	Component	Salinity change	Component	Temperature change [°C]
Total	Total	-0.220	Total	-0.95
Transit	Transit	-0.025	Transit	1.00
Labrador Sea	Volume	-0.135	Volume	-1.10
	Salinity	0.015	Temperature	-0.05
Gulf Stream	Volume	-0.060	Volume	-0.40
	Salinity	-0.020	Temperature	-0.30
Other	Volume	-0.010	Volume	0.00
	Salinity	0.000	Temperature	0.00

We now quantify the contributions of each of the variables on the RHS (right-hand side) of Eq. 7 to changing properties of water crossing $OSNAP_{E\text{-}37W\text{-}500m}$ during the period of most rapid freshening and cooling, between 2011-12 and 2016-17 (Table 1). For salinity, over 60 % of the freshening is due to increasing volumes of water from the Labrador Sea, and 27 % due to decreasing volumes from the Gulf Stream. The small remainder is a combination of along-track external fluxes and changes in TS properties in the origin regions, particularly slight freshening of the Gulf Stream origin. For temperature the picture is more complicated, half of the overall mean cooling of water leaving the combined origin regions is mitigated along-track by reduced heat loss from the cooler water. The net all-source mean cooling of water leaving the origin regions is, as for salinity, driven mostly by increasing volumes of water from the Labrador Sea (over 55 %) and decreasing volume of water from the Gulf Stream (20 %). As for freshening, a small contribution to the cooling at $OSNAP_{E\text{-}37W\text{-}500m}$ stems from temperature changes at the sources, specifically, from a reducing mean temperature of waters leaving the Gulf Stream origin.

It is important to note that in the later years modelled, when volume transports of Gulf Stream origin are below their 30-year mean and those of Labrador Sea origin above their mean, our analysis underestimates the influence of Labrador current origin transports on $OSNAP_E$ properties and overestimates the influence of Gulf Stream origin transports. However, this only further stresses the importance of the described changes in the Labrador Sea for the development of the recent eastern cold and fresh anomalies.

https://doi.org/10.5194/os-2022-18
Preprint. Discussion started: 11 April 2022

4.4 Summary of particle tracking results

We find only small changes in the modelled TS properties of the Gulf Stream and the Labrador Sea origin waters as they leave their respective source regions and also no substantial freshening or cooling through along-track changes. Hence, the exceptional freshening and cooling in the eastern subpolar North Atlantic is driven by the increasing proportion of fresher Labrador Sea origin waters in the mix compared to saltier Gulf Stream origin waters. We have not identified any rapid – annual or intra-annual – changes in source properties, transports or pathways driving the freshening and cooling, but rather pentadal to decadal, persistent changes beginning in the early 2000s. The increasing volume of Labrador Sea origin water accounts for over 60 % of the freshening, in combination with reduced transport from the Gulf Stream accounting for about 30 %. For temperature, the shift in relative proportions of water from the two main sources drives the cooling, but the average cooling of the combined-source waters is mitigated (reduced by about half) by reduced heat loss along-track.

In the following sections, we explore and discuss the possible mechanisms responsible for the modelled changes in the quantities and proportions of waters transported northwards through the eastern subpolar North Atlantic from the two major sources identified.

5 Mechanisms

5.1 North Atlantic Current changes and SPG eastward expansion

The distribution of transit times for particles to travel from the source to $OSNAP_{E\text{-}37W\text{-}500m}$ (Fig. 4a) show shortest times of under a year and a distribution mode of about 2 years. The distributions are skewed right, with a long tail out to longer transit times. The transit time distributions have a similar shape for all sources and years, with a steep early rise and long tail at longer transit times, so we can characterise transit time variability by examining variability in the mean. We find contrasting evolution of transit times for particles crossing $OSNAP_{E\text{-}37W\text{-}500m}$ in the east (Rockall-Hatton Bank and Rockall Trough) and west (Iceland Basin and Irminger Sea), so we split the section at 21° W (Fig. 8).

In the east, over Rockall-Hatton Bank and in the Rockall Trough, northward transports are dominated throughout by waters of Gulf Stream origin. Some increase in transports is seen after 2004 (Fig. 8b) as Gulf Stream source waters are increasingly confined to this eastern section in the later half of the period studied. Transit times, speeds and track lengths to this eastern section of $OSNAP_{E\text{-}37W\text{-}500m}$ from the individual sources show little consistent change over time (Fig. 8d,f,h) except for a slight slowing of the loop path (though volumes on this path are very small).

In the Iceland Basin and Irminger Sea, across $OSNAP_{E\text{-}37W\text{-}500m}$ west of 21° W, the Gulf Stream influence reduces steadily between 2004 and 2016 and is largely replaced by direct path waters from the Labrador Sea (Fig.8a). Mean transit times in the west, from all sources, increase by around 30 % between 1998 and 2016 (Fig.8c). This is due to a combination of reduced current speeds and increasing track lengths (Fig.8e,g). The increasing track lengths result from eastward shift of the mean $OSNAP_{E\text{-}37W\text{-}500m}$ crossing longitudes (Fig.8i) and increased along-track eddying (results supported by Eulerian analysis of

https://doi.org/10.5194/os-2022-18
Preprint. Discussion started: 11 April 2022

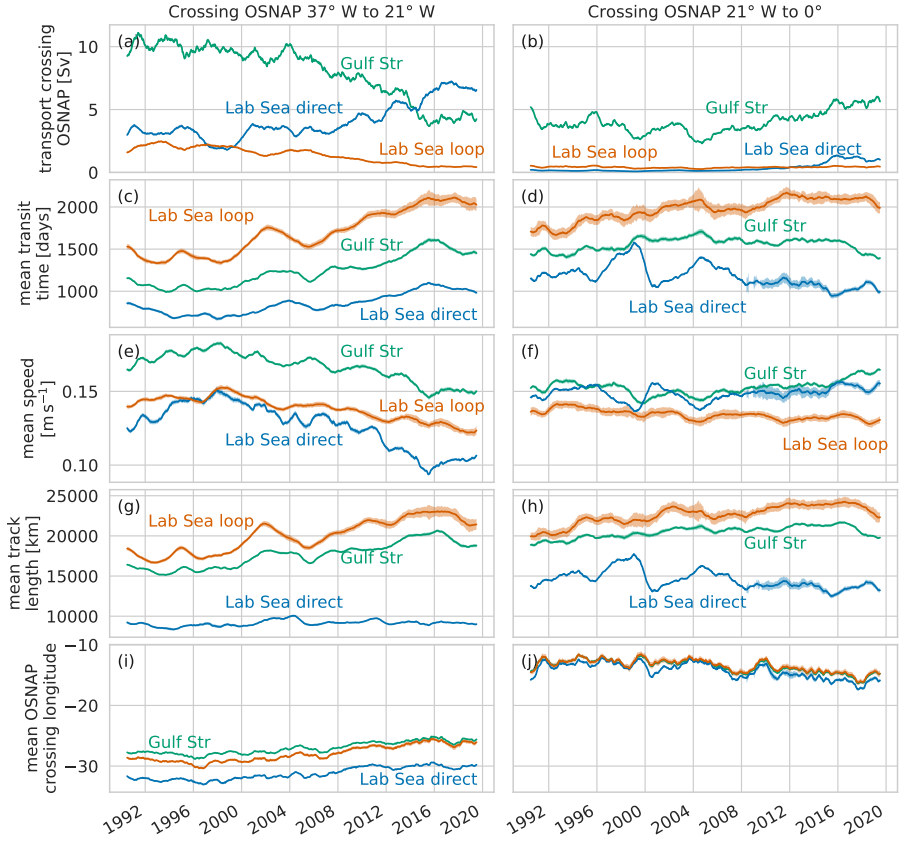

Figure 8. Evolution over time of particle transit times. Time series of mean volume transports **(a,b)**, transit times **(c,d)**, speeds **(e,f)**, track lengths **(g,h)** and $OSNAP_{E\text{-}37W\text{-}500m}$ crossing longitude **(i,j)** of particles by source. Results are divided into regions west (left column) and east (right column) of 21° W, the western flank of the Rockall-Hatton Bank. Times on the x-axis are crossing times of $OSNAP_{E\text{-}37W\text{-}500m}$, so values represent weighted averages of conditions along-track in the preceding years. Time series are smoothed with a 1-year rolling mean.

VIKING20X NAC, not shown). After 2016 transit times from all sources to $OSNAP_{E\text{-}37W\text{-}500m}$ west of 21° W start to decrease, with faster speeds and shorter paths recorded, perhaps associated with a strengthening subpolar gyre from 2013.

These results are consistent with an eastward expansion of the SPG between 2006 and 2016, with the reduced volumes of Gulf Stream origin surface waters increasingly confined to the east, passing $OSNAP_{E\text{-}37W\text{-}500m}$ over Rockall-Hatton Bank and Rockall Trough. The Irminger Sea and Iceland Basin sections of $OSNAP_{E\text{-}37W\text{-}500m}$ are correspondingly increasingly dominated by waters from the Labrador Sea.

Changing current speeds and pathways in the SPG and NAC have been linked to eastern subpolar North Atlantic freshening (Bersch, 2002; Sarafanov, 2009; Bersch et al., 2007; Hátún et al., 2005; Koul et al., 2020). The proposed mechanism is that eastward expansion and strengthening of the SPG regulates northward transport of warm salty water from the subtropics, modulating the proportion of subpolar and subtropical waters reaching the eastern North Atlantic (Häkkinen et al., 2011).

https://doi.org/10.5194/os-2022-18
Preprint. Discussion started: 11 April 2022

Using a subpolar gyre index (SPGI) based on the second principal component of sea surface height variability (Koul et al., 2020), Biastoch et al. (2021, Fig. 10) show a weak SPG in VIKING20X from 1996–2012, with increasing strength from 2013. Here we find that, while reduced salinity in the upper eastern subpolar North Atlantic is due to an increasing proportion of subpolar waters, this freshening, starting as early as 2008, appears to lead the increase in SPG strength. We can compare the late 2010s with the previous strong SPG of the early 1990s during which VIKING20X shows an increased SPGI (Biastoch et al., 2021, Fig. 10) but a much smaller increase in the proportion of subpolar water at $OSNAP_E$ (Fig. 5 and correspondingly smaller cooling and freshening signal in the combined source TS (Fig. 7a,b.

SPG decadal-scale dynamics are complex and still poorly understood. Häkkinen et al. (2011); Chafik et al. (2019) observe that a strong SPG during periods of eastern subpolar North Atlantic cooling is associated with a strengthened wind-stress curl, a horizontally expanded gyre, a southeastwards shifted NAC pathway, and reduced advection of warm and saline subtropical waters into the northeast Atlantic. Alternatively, Robson et al. (2016) propose that cooling of the upper eastern subpolar North Atlantic is due to reduced transport of warm water from the south associated with decreased AMOC, which in turn is linked to record low densities (lighter water) in the deep Labrador Sea.

The VIKING20X model results, we present here, suggest a decoupling of the eastward expansion of the SPG from the strength, with eastward expansion observed during a period of weaker SPG. The cooling we observe in transports at $OSNAP_{E\text{-}37W\text{-}500m}$ beginning before 2012 is mainly linked to an increasing proportion of subpolar water (Fig. 7), which is comprised of increasing volumes of water which left the Labrador Sea from around 2008 (Fig. 5).

While we cannot discount SPG variability – linked to wind-stress curl and Ekman dynamics – from contributing to the exceptional cooling, the upstream trends in transports, which drive the freshening and cooling in the eastern subpolar North Atlantic, begin before 2008 in a period of weak – and possibly still weakening (Biastoch et al., 2021, Fig. 10) – SPG. Below we further explore the contribution of reduced northward flow from the subtropics (basin-scale mechanisms) and, somewhat analogous to Robson et al. (2016), processes upstream of the Labrador Sea outflow (subpolar gyre-scale mechanisms), to the exceptional freshening event.

5.2 Basin-scale mechanisms - overturning

Observational analyses, for example from the RAPID Meridional Overturning Circulation and Heat-flux Array (RAPID-MOCHA) (Cunningham et al., 2007) and application of the Bernoulli inverse to hydrography (Fraser and Cunningham, 2021), show weakening AMOC during our experiment period. The AMOC in VIKING20X shows a similar weakening at latitudes throughout the North Atlantic (Biastoch et al., 2021).

We here show results at 29° N (Fig. 9), a latitude close to the RAPID observation line and to our Gulf Stream source definition latitude. At 29° N in VIKING20X-JRA-short, the Gulf Stream flow (defined here as the northward flow on the shelf) weakens between 1990 and 2020, accompanied by a reduced AMOC. The remainder, subtropical gyre recirculation, shows no overall trend. So the Gulf Stream weakening is associated with reduced flow northwards from the subtropical towards the subpolar North Atlantic in the upper layers and corresponding reduced deep return flow – that is reduced AMOC. This weakening

https://doi.org/10.5194/os-2022-18
Preprint. Discussion started: 11 April 2022

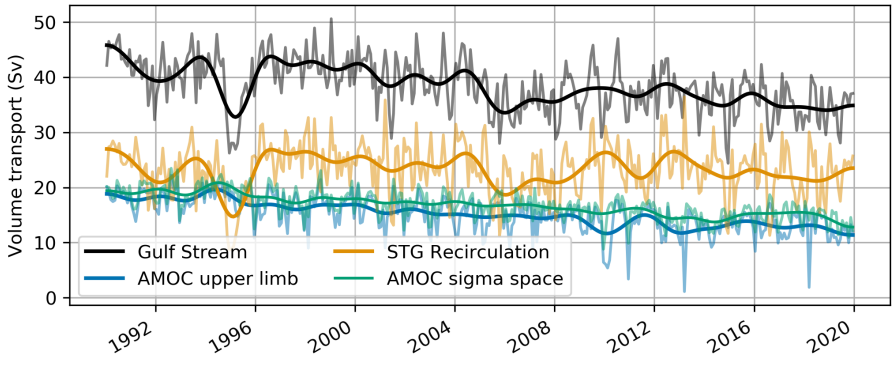

Figure 9. Northward transports and AMOC strength at 29° N in VIKING20X. Pale lines are monthly mean data, darker lines are low-pass filtered using a Butterworth filter and 18 month cut-off. The total transport in the Gulf Stream (black line) reduces throughout the experiment duration, while the volume recirculating in the subtropical gyre above 1000 m (light orange line) shows a smaller trend or remains largely constant. This implies weakened AMOC and reduced northward flow in the AMOC upper limb (blue, AMOC in z-space). At 29° N, the AMOC in σ-space (green) is very similar to $AMOC_z$ and also reduces consistently. The reducing AMOC strength closely reflects the reducing contribution of Gulf Stream source transport found from the particle tracking.

AMOC, by about 30 %, is responsible for the reduction in transport from the Gulf Stream to $OSNAP_E$ between the 1990s and 2016 (Fig. 5) diagnosed by the Lagrangian tracking.

Previous longer-term, lower-resolution modelling work (Koul et al., 2020) linked periods of higher subpolar gyre index to weaker flow from the subtropical gyre to the NAC, suggesting a possible 'blocking' mechanism. But, the AMOC weakening in VIKING20X between 1990 and 2020 appears to be independent of the subpolar gyre strength. In this period the AMOC is weakening contrasting with a high (1990s) to low (2000s) to high (late 2010s) cycle in the subpolar gyre index.

Examination of the decadal scale drivers of the AMOC, in either the real ocean or in VIKING20X is beyond the scope of the current work, but we refer the reader to Biastoch et al. (2021) for a detailed analysis. They find outflow of deep water from the Labrador Sea at 53° N to be a good indicator of the subpolar AMOC trend and also a strong dependence on the choice of freshwater forcing in the model. The VIKING20X-JRA-short run used here shows a stronger decline in the AMOC than either observations or other VIKING20X realisations since 1990, but all consistently suggest a decline for this period.

Comparing the VIKING20X AMOC time series since 2005 with the observational time series from RAPID (Bryden et al., 2020, Fig. 1), in VIKING20X the AMOC appears 2–3 Sv too weak but the model reproduces the observed decline in overturning and also the minimum in overturning in winter 2009-10. This minimum is suggested in Bryden et al. (2020) as the start of a period of reduced northward transport of heat and salt from the subtropics to the subpolar gyre. These similarities between model and observations give us confidence that we are, at least qualitatively, reproducing the contribution of changes in overturning circulation to reduced eastern North Atlantic salinity and temperature. If anything, VIKING20X overestimates the AMOC decline and may therefore overestimate the role of the AMOC weakening in the observed eastern subpolar gyre freshening and cooling.

https://doi.org/10.5194/os-2022-18
Preprint. Discussion started: 11 April 2022

In summary, we find little evidence that a slowing AMOC was a dominant contributor to the 2012-2016 freshening. In VIKING20X we see a gradual decline in subtropical water transported across $OSNAP_{E\text{-}37W\text{-}500m}$ between the mid-1990s and 2016, contrasting with the accelerating freshening and cooling from 2011–2016. Reduced subtropical transports will amplify TS variability in the eastern subpolar North Atlantic due to variability in subpolar gyre transport from the Labrador Sea (Eq. 7).

5.3 Subpolar gyre-scale mechanisms

5.3.1 Pathways from the Labrador Sea

Upper water from the Labrador Sea reaches the eastern subpolar North Atlantic along one of two dominant pathways (Holliday et al., 2020; New et al., 2021): a direct pathway, and a loop pathway which follows the coast southwestwards through the Slope Sea north of the Gulf Stream before reversing, joining the Gulf Stream source waters travelling to the northeast (Fig. 3d,e. A change in the dominance of the direct pathway for cold fresh Arctic water from the Labrador Current has been offered as a cause of the exceptional freshening event (Holliday et al., 2020).

Examining the changing volume transports along these two pathways between the Labrador Sea (Fig. 5) and $OSNAP_{E\text{-}37W\text{-}500m}$ shows the ratio of the direct to loop source volume changes from close to 1:1 before 2000, to 8:1 after 2016. Prior to 2006, dominance switches repeatedly between the two pathways with little change in total transport (Fig. 5b). This early period supports the ideas of changing pathway dominance of Holliday et al. (2020), but after 2006 the net increase in volumes leaving the Labrador Sea towards $OSNAP_{E\text{-}37W\text{-}500m}$ in VIKING20X is entirely along the direct path.

It is this more recent increase in total volume of Labrador Sea source water, rather than by the details of pathways taken, which we showed in Section 4 is responsible for the major part of 2012–2016 freshening and cooling in the eastern subpolar North Atlantic. In the following sections we explore possible mechanisms driving this increased total transport from the Labrador Sea.

5.3.2 Labrador Sea upstream sources

Increased transport from the Labrador Sea must be associated with changes in transport from sources upstream of the Labrador Sea outflow. Tracking the Labrador Current source water particles back in time, further upstream (Fig. 10), we can distinguish between four sources: Hudson Bay; the Davis Strait; from the Greenland Sea, southward across the Greenland–Scotland ridge; and SPG water (particles circulating in the SPG, and having previously passed northwards across $OSNAP_E$). These source definitions closely correspond to the definitions of Hudson outflow, LC-Arctic (Labrador Current-Arctic, our Davis Strait source) and LC-Atlantic (Greenland Sea and SPG recirculation) water used in Florindo-López et al. (2020); Holliday et al. (2020); New et al. (2021)).

The overall increase in volume of Labrador Sea origin water (4 Sv) is primarily originating from an increase in circulating SPG (or LC-Atlantic) water (3 Sv) with a smaller contribution from increases in Greenland Sea and Davis Strait (or LC-Arctic) source waters (1 Sv). While volumes taking the direct path increase and those taking the loop path decrease, we find little variability, and no trend, in the percentage composition of the water forming either the direct or loop paths. The direct path

https://doi.org/10.5194/os-2022-18
Preprint. Discussion started: 11 April 2022

Ocean Science
Discussions
Open Access
EGU

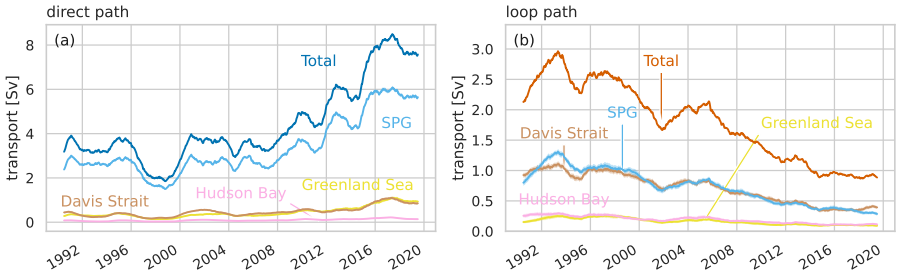

Figure 10. Labrador Current upstream sources. Quantifying contributions from upstream sources of the Labrador Current for the direct path ((**a**) and the loop path (**b**)). Upper layer inflow to the Labrador Sea comes from Hudson Bay (pink), Davis Strait (brown) and in the West Greenland Current. The West Greenland Current is further divided here into water from the Greenland Sea (yellow) and recirculating SPG water (light blue). There is little change in the proportions of water from different upstream sources forming the different paths (loop or direct). Overall, the increased contribution of the direct path **(a)** is reflected in an increase in the total volume of recirculating SPG transport and a small increase in the total contribution from the Greenland Sea. Particles from Hudson Bay, Davis Strait, and the Greenland Sea have come directly from those regions, SPG waters are circulating in the subpolar gyre and have previously crossed northwards across OSNAP_{E}.

is about 80 % SPG water, 10 % Davis Strait and 10 % Greenland Sea; the loop path is 40 % SPG, 40 % Davis Strait, 10 % Greenland Sea and 10 % Hudson Bay. All the flows we are examining here are in the light, upper layers.

There is little change in total volume contribution from Hudson Bay or from Davis Strait sources, although the dominant pathway taken by the Davis Strait source water switches from loop to direct. This is exactly the switch of dominance described by Holliday et al. (2020) for LC-Arctic water.

The small increase in contribution of upper waters from the Greenland Sea is interesting, perhaps suggesting increased Greenland meltwater flowing southward in the East Greenland Current. The fate of this fresh water in regions of deep water formation has led to speculations that the accelerating melting of the Greenland Ice Sheet could stratify the subpolar gyre, change the spatial deep convection patterns, and slow or stop the AMOC (see for example Böning et al., 2016; Foukal et al., 2020; Rühs et al., 2021). But this increase accounts for <20 % of the increase in transport from the Labrador Sea to $\text{OSNAP}_{\text{E-37W-500m}}$.

The largest part ∼75 %, 3 Sv, of the increased transport from the Labrador Sea is due to increased volumes remaining longer and recirculation within the upper North Atlantic subpolar gyre (LC-Atlantic water). This recirculation doubles, from 3 to 6 Sv, between the early 2000s and 2016, representing an increase from ∼15 % to ∼30 % of the northward transport across $\text{OSNAP}_{\text{E-37W-500m}}$. It is this recirculation which is driving the increase in transport from the Labrador Sea to $\text{OSNAP}_{\text{E-37W-500m}}$, and in turn the freshening and cooling.

Note that we do not necessarily associate this increased recirculation with a stronger SPG, but rather with reduced conversion rates to denser water and so increasing residence times for water in the upper water of the subpolar gyre. Upper layer waters in the subpolar North Atlantic generally enter from the subtropics; they are then cooled and freshened (and made denser) by surface fluxes, ice-ocean interaction and inputs from the land, either in the subpolar ocean or the Arctic seas; before leaving

https://doi.org/10.5194/os-2022-18
Preprint. Discussion started: 11 April 2022

the upper ocean as denser intermediate water masses (for example Labrador Sea Water (LSW), some retained in the subpolar region and some exported southwards) and deep water masses (exported southwards in the deep currents). Longer subpolar residence times suggest a weakening of these densification processes in the upper subpolar and/or Arctic seas. We will return to this idea later on (see Section 6).

5.3.3 Labrador Sea outflow

A VIKING20X mean velocity section across the shelf and shelf break at the western end of the $OSNAP_W$ line spans the upper layer outflow, the Labrador Current, the source region of all the modelled transport from the Labrador Sea to $OSNAP_{E\text{-}37W\text{-}500m}$ (Fig. 11a). This shows upper layer outflow to be concentrated in two main cores: one close to the coast – Labrador Coastal Current, Hudson outflow and some LC-Arctic water; and the other (larger and stronger) over the shelf break. This offshore current can be separated (see Florindo-López et al., 2020) into distinct shallower (upper 200 m) inshore (of the 600 m isobath) LC-Arctic and deeper offshore LC-Atlantic components. Most of the water exiting the Labrador Sea with a density (σ_0) lighter than 26.65–26.70 $\mathrm{kg\,m^{-3}}$ is transported round to $OSNAP_{E\text{-}37W\text{-}500m}$ in the surface 500 m.

Pentadal mean velocity anomalies (Fig. 11b–g) across this Labrador Sea outflow section show no coherent overall increase in outflow velocities (negative, blue, in Fig. 11(b)-(g))velocities. The anomalies in the LC-Arctic outflow are entirely consistent with Florindo-López et al. (2020), showing higher outflow in the early 1990s and late 2010s and reduced outflow between. This indicates a change in the freshwater transport into the subpolar North Atlantic of that current, but the total LC-Arctic outflow (mostly Davis Strait Greenland Sea water in Section 5.3.2) is typically less than 2 Sv (New et al., 2021), so the increased outflow after 2005 forms a minor component of the total outflow increase, which is dominated by the offshore LC-Atlantic, SPG water.

Pentadal mean density fields do show deepening of all isopycnals between 27.60 $\mathrm{kg\,m^{-3}}$ and 27.75 $\mathrm{kg\,m^{-3}}$ between the 1990–94 and 2010–2014 pentads (Fig. 11b—g). There is a slight recovery to shallower depths by 2015–2019. It is the resulting increase in the cross-sectional area occupied by outflowing lighter waters, rather than increased flow speeds, which produces the increased transports of light waters out of the Labrador Sea.

Notice that there is no obvious increase or decrease in cross-sectional area occupied by the very lightest waters (σ_0 <27.50 $\mathrm{kg\,m^{-3}}$). These waters of the Labrador Coastal Current, combined with some LC-Arctic water from the shelf break, mainly follow the loop path. Labrador Current outflow along the loop path has been found to be related to Gulf Stream transport and AMOC strength (New et al., 2021; Sanchez-Franks et al., 2016) possibly via wind stress in the subpolar gyre.

So, qualitatively, we see the potential for increasing volume transport from the Labrador Sea to the upper eastern subpolar North Atlantic to be due to a deepening of the surface layer of lighter water in the Labrador Sea rather than faster currents. We now explore that idea further, examining the sources of the increasing outflow of lighter waters, using a water mass transformation budget in the Labrador Sea Walin (1982); Speer and Tziperman (1992).

https://doi.org/10.5194/os-2022-18
Preprint. Discussion started: 11 April 2022

Ocean Science
Discussions
Open Access
EGU

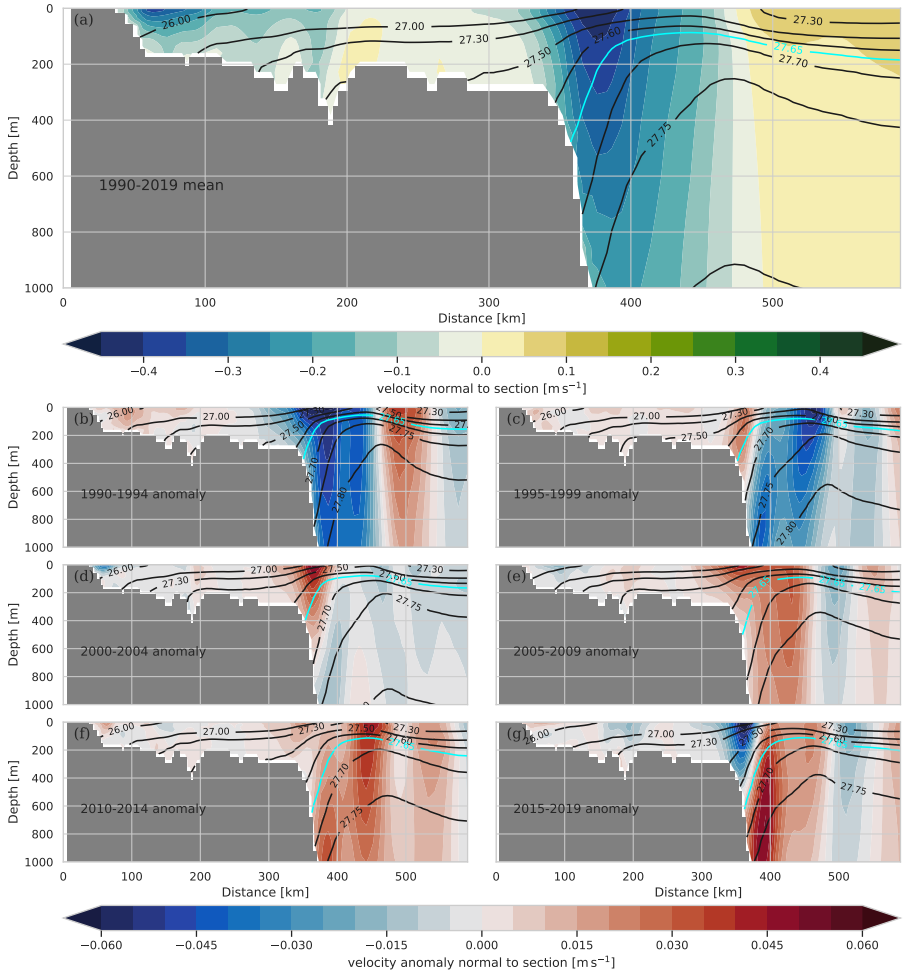

Figure 11. Vertical sections of Labrador Sea upper layer outflow 1990–2019 mean velocity **(a)** and pentadal velocity anomalies from the mean **(b)–(g)**, with period-mean density contours superimposed, at the western end of the OSNAP line. Velocities, and velocity anomalies, are shown as positive into the Labrador Sea. Lighter waters (<27.65 $\mathrm{kg\,m^{-3}}$) leaving the Labrador Sea are mostly transported to $\mathrm{OSNAP_E}$ in the subpolar gyre, this transport is dominated by strong currents at the shelf break. Outward currents in the lighter density classes are weaker (positive – red – anomalies) than the 30-year average between 2000 and 2015 (**(d)-(f)**). The increasing contribution of Labrador Sea source waters to eastern SPG transports in the 2010s is associated with deepening of these lighter layers rather than increasing currents, notice the highlighted 27.65 $\mathrm{kg\,m^{-3}}$ isopycnal in panels **(b)–(g)**.

https://doi.org/10.5194/os-2022-18
Preprint. Discussion started: 11 April 2022

6 Labrador Sea water mass analysis

6.1 Full water mass balance

To first order, the Labrador Sea is fed by water from the West Greenland Current, through the Davis Strait, from Hudson Bay together with river, meltwater and precipitation inflows; this water is transformed to denser water within the Labrador Sea by winter cooling and ice formation before exiting southwards via the Labrador Current in the upper ocean and the DWBC below.

The mean water mass transformations (Walin, 1982; Speer and Tziperman, 1992) on the ocean model volume bounded by OSNAP_W, Davis Strait at 67° N and the exit of Hudson Bay at 68° W (Fig. 12) confirm this balance. On average, net boundary inflow (inflow - outflow) acts to increase the volume of water lighter than $\sigma_0 = 27.70\,\text{kg}\,\text{m}^{-3}$, and reduce the volume of denser waters. This net inflow is primarily balanced by the surface heat loss, cooling the lighter inflow waters and hence transforming them to higher densities before they flow out of the Labrador Sea. The contribution to transformation by surface freshwater fluxes (including river inflow, ice melt/formation and precipitation-evaporation) is much smaller than the cooling. There is also a small change in the relative volumes of water within the Labrador Sea, with increasing volumes of waters in most density classes balanced by decreasing volumes of the densest waters.

6.2 Changing water mass balance in the upper Labrador Sea

From water mass transformation theory we know that the net rate of inflow water $\rho < \rho_0$ is balanced by the rate of change of volume with $\rho < \rho_0$ and the rate of transformation of water across the $\rho = \rho_0$ isopycnal. This transformation rate is a function of the surface heat and freshwater flux at $\rho = \rho_0$ isopycnal outcrop, and the transformation by interior mixing across the $\rho = \rho_0$ surface. Figure 13 shows how this balance evolves over time for lighter waters of $\sigma_0 < 27.65\,\text{kg}\,\text{m}^{-3}$. We also further split the net inflow into 'inflow' and 'outflow' components by assuming the inflows to be through Davis Strait, Hudson Bay, and across OSNAP_W north of 57° N (mostly the west Greenland Current), and all outflow to occur across OSNAP_W south of 57° N. It is the variation in time of this 'outflow' in the southern half of OSNAP_W we are interested in.

The $\sigma_0 = 27.65\,\text{kg}\,\text{m}^{-3}$ density level is chosen because, in VIKING20X, it represents the approximate density lighter than which most water exiting the Labrador Sea is transported across to OSNAP_E in the upper layer. Coincidentally, it is close to the division between the upper and lower limbs of the meridional overturning at the OSNAP line. We will use 'upper limb water' and 'lower limb water' as shorthand for water lighter and denser than $\sigma_0 = 27.65\,\text{kg}\,\text{m}^{-3}$, respectively. The precise choice of density level, between $\sigma_0 = 27.65\,\text{kg}\,\text{m}^{-3}$ and $\sigma_0 = 27.70\,\text{kg}\,\text{m}^{-3}$, does not affect the conclusions. The density $\sigma_0 = 27.70\,\text{kg}\,\text{m}^{-3}$ is often considered to be the lighter density limit of the deeper LSW intermediate water masses in the North Atlantic.

On interannual and longer timescales, after 2000, the modelled inflow of upper limb water to the Labrador Sea shows some variability but no trend. The outflow of these waters after 2000, while always being less than the inflow, has an increasing trend (Fig. 13a) closely resembling the timing of, but of slightly larger amplitude than, the increase of the Labrador Current source transport observed in the particle tracking. The amplitude difference is because there is not a 1:1 correspondence between Labrador Sea outflow $\sigma_0 < 27.65\,\text{kg}\,\text{m}^{-3}$ and water parcels tracked to $\text{OSNAP}_{\text{E-37W-500m}}$.

https://doi.org/10.5194/os-2022-18
Preprint. Discussion started: 11 April 2022

Ocean Science
Discussions
Open Access
EGU

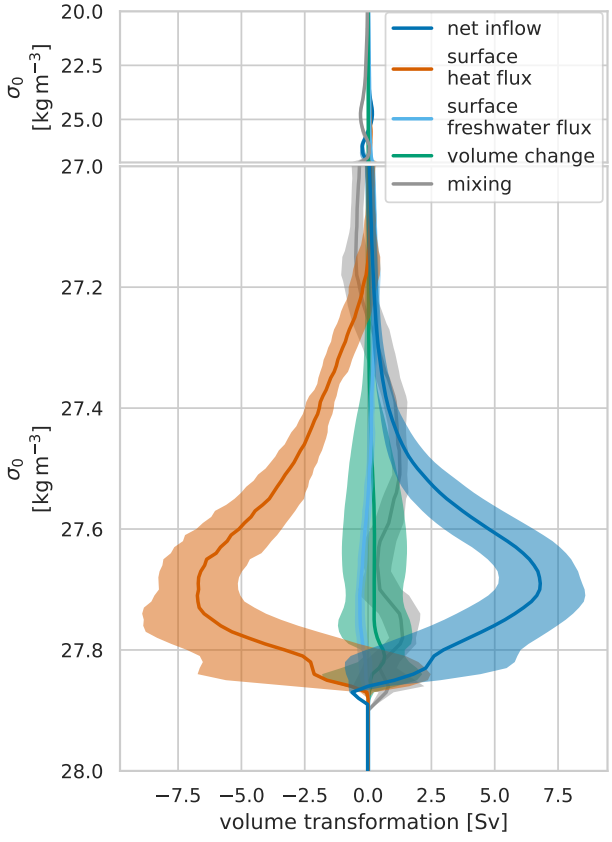

Figure 12. VIKING20X Labrador Sea mean water mass balance. Positive values of volume transformation are transformations across the isopycnal towards lighter densities. Net production of water of a particular density is therefore shown as negative gradients and net removal as positive gradients (i.e. surface heat flux acts to remove lighter waters by cooling – positive gradients – producing denser waters – negative gradients). The primary balance is between net inflow of lighter water and conversion to denser water by surface heat flux. Solid lines are average annual mean transformations, 1990-2019, shaded area shows ± 1 standard deviation in the annual mean.

Hence the decline in net inflow (difference inflow-outflow) of these upper limb waters after the year 2000 is the result of increasing outflow and must be balanced either by reduced transformations across the $\sigma_0 = 27.65\,\mathrm{kg\,m^{-3}}$ isopycnal or a reduction in the volume of water $\sigma_0 < 27.65\,\mathrm{kg\,m^{-3}}$ (negative volume tendency) in the Labrador Sea (Fig. 13b). On these multiyear timescales, the declining net inflow (and therefore the increasing Labrador Sea outflow) of upper limb waters is found to be due to reduced transformation to denser layers by surface heat flux (i.e. reduced cooling) along the $\sigma_0 = 27.65\,\mathrm{kg\,m^{-3}}$ isopycnal outcrop. The contributions from volume tendency, freshwater flux (Fig. 13b) and diapycnal mixing are smaller.

Prior to 2000, there is a period of increasing inflow of upper limb waters in the West Greenland Current (Fig. 13a). This increase is balanced by increasing transformation to lower limb densities within the Labrador Sea by surface heat flux, resulting in little change in outflow of upper limb waters.

https://doi.org/10.5194/os-2022-18
Preprint. Discussion started: 11 April 2022

Ocean Science
Discussions
Open Access
EGU

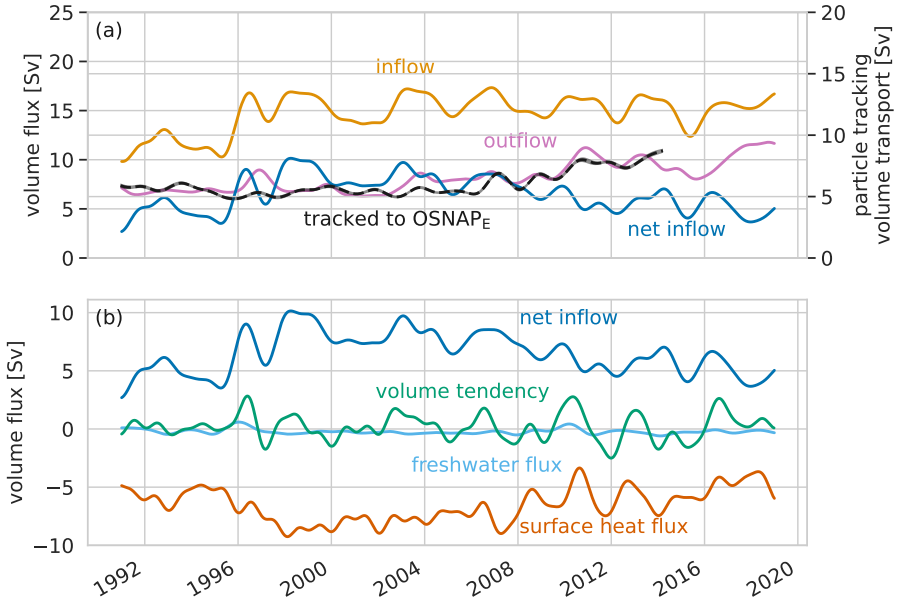

Figure 13. Labrador Sea water mass balance time series for $\sigma_0 < 27.65\,\mathrm{kg\,m^{-3}}$. The inflow (**(a)**, light orange) shows no clear trend after 1998, whereas the outflow (**(a)**, purple) shows a clear increase. Summing inflow and outflow shows a reducing net inflow of lighter waters to the Labrador Sea after 1998 (blue line, **(a,b)**). The transport leaving the Labrador Sea, heading to OSNAP$_{\text{E-37W-500m}}$, from the particle tracking is included in **(a)** (dashed black line) for comparison. Note the slightly different scale on the right hand y-axis for this line to help comparison since there is not a 1:1 correspondence between water $\sigma_0 < 27.65\,\mathrm{kg\,m^{-3}}$ leaving the Labrador Sea and water tracked to OSNAP$_{\text{E-37W-500m}}$). In **(b)**, this reduced net inflow of light water must be balanced by water mass volume transformations – heat flux out of the ocean (orange/red line), freshwater flux (light blue) – or show as changing volume in the volume tendency term (green). Time series are generated from 5-day VIKING20X output lowpass filtered with a butterworth filter and 18 month cutoff.

In summary, in the VIKING20X model results we have shown reduced cooling in the Labrador Sea leading to increased transport of lighter upper waters out of the Labrador Sea. This increased transport, when mixed with the warmer, saltier waters of Gulf Stream origin in the NAC, increases the relative contribution of fresher, cooler Labrador Sea origin waters and acts to freshen and cool the transports through the eastern subpolar North Atlantic.

6.3 Comparison with observations

Finally, we return to comparison between VIKING20X and the EN4 data and examine the deepening isopycnals in the Labrador Sea which in Section 5.3.3 we propose as the mechanism whereby increasing volumes of lighter waters exit the Labrador Sea.

The volume tendency term for lighter waters in the Labrador Sea water mass transformation analysis is comparatively small each year (Fig. 13). But, over time it accumulates into a notable deepening of the upper Labrador Sea average annual mean isopycnal depths. Between the early 1990s and about 2014-16, the annual mean depth of isopycnals in the range $\sigma_0 = 27.65$–

https://doi.org/10.5194/os-2022-18
Preprint. Discussion started: 11 April 2022

$27.80\,\mathrm{kg\,m^{-3}}$ almost doubles (Fig. 14f). After 2014, with resumption of deeper convection in the Labrador Sea, the annual mean isopycnal depths begin to decrease. Examination of the associated average modelled temperature and salinity profiles (Fig. 14d,e) show the isopycnal deepening to be the result of warming of the waters below $200\,\mathrm{m}$. This is consistent with the results of the water mass analysis above which identified surface heat fluxes as the driver of increased outflow of lighter waters from the Labrador Sea.

The modelled Labrador Sea isopycnal depths described here agree closely with observations from both the EN4 dataset (Fig. 14a–c) in the Labrador Sea and from Fisheries and Oceans Canada (DFO) ship-based surveys and Argo floats reported in Yashayaev and Loder (2017). For LSW (Labrador Sea Water), typically the intermediate water mass (approximately $\sigma_0 =$ 27.74–$27.80\,\mathrm{kg\,m^{-3}}$) immediately below the upper layer waters we are interested in here, the detailed repeat observations of Yashayaev and Loder (2017) show cumulative surface heat fluxes in the Labrador Sea after the early 1990s leading to increased temperatures in the depth range 200–$2000\,\mathrm{m}$ (Yashayaev and Loder, 2017, Fig. 3), and resulting in the 2012—2016 LSW class being one of the deepest and most persistent ever observed.

Both model and EN4 Labrador Sea temperature changes clearly show the warming of the water in the 200–$2000\,\mathrm{m}$ depth range up to 2012 (Fig. 14b,e). The salinity and density comparisons are less convincing, but EN4 data appear to have some anomalously fresh salinity values to large depths, particularly prior to year 2000, the start of the Argo float era. These anomalous salinity values feed into the density values, making the temperature comparison the most reliable.

These model-data comparisons of Labrador Sea temperature, salinity and density structures show that the model is evolving realistically and support the proposed mechanism, of reduced heat loss over a period of years leading to deepening upper layer isopycnals in the Labrador Sea and to increased outflow of lighter upper layer waters.

7 Conclusions

We have used the high-resolution eddy-rich nested ocean–sea-ice model VIKING20X to explore the causes of the exceptional freshening (and cooling) event observed in the surface 500–$1000\,\mathrm{m}$ of the eastern subpolar North Atlantic in the years from 2012 onwards. We find a major factor to be reduced surface heat loss from the Labrador Sea during the decade preceding the exceptional freshening, which is perhaps counter-intuitive.

Surface heat loss in the Labrador Sea transforms lighter inflow from the West Greenland Current to denser water which flows out in the Labrador Current system. But not all the light surface inflow water is converted to denser intermediate and deep water, some flows out of the Labrador Sea in the upper few hundred metres at densities $\sigma_0 < 27.65\,\mathrm{kg\,m^{-3}}$. Reducing heat loss in the Labrador Sea therefore can lead to increased volumes of lighter waters remaining in the upper layers, deepening the isopycnals and increasing the outward transport of lighter upper layer waters in the Labrador Current system.

The relatively fresh and cold upper layer waters flowing out of the Labrador Sea combine with warmer saltier upper layer waters from the subtropics. They then form the upper waters of the eastern subpolar North Atlantic together. The TS characteristics of the resulting waters are largely governed by the ratio of volumes of water from the two major sources in the mix.

https://doi.org/10.5194/os-2022-18
Preprint. Discussion started: 11 April 2022

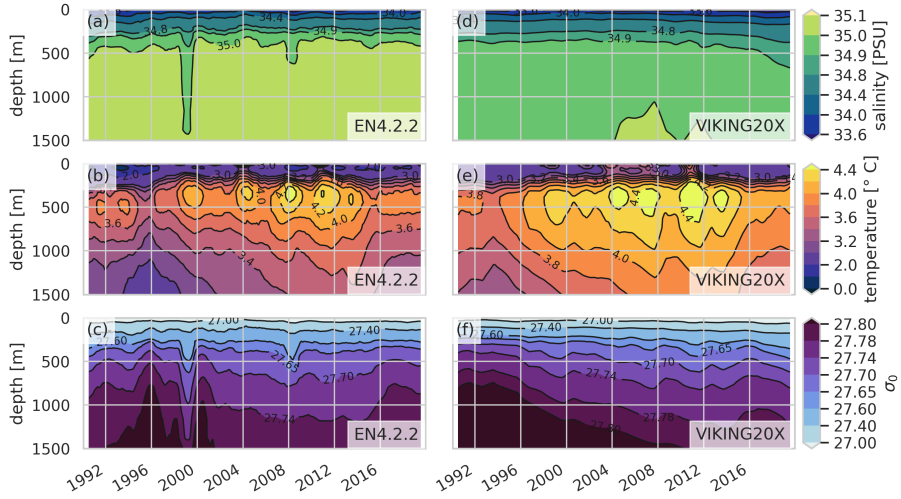

Figure 14. Evolution of the vertical structure of annual mean, basin mean salinity, temperature and σ_0 in the Labrador Sea between $OSNAP_W$ and the Davis Strait, from EN4.2.2 data **(a)–(c)** and VIKING0X **(d)-(f)**. The development of warmer subsurface waters in both observations and data between the late 1990s and 2016, peaking around 2012, is seen. The model is slightly biased towards warmer, fresher water at all depths.

In this way reduced Labrador Sea surface heat loss, and resulting outward transport increased volumes of lighter upper layer waters from the Labrador Sea, is found to lead to freshening and cooling downstream in the eastern subpolar North Atlantic.

The quantitative particle tracking allows us to estimate contributions to the exceptional freshening and cooling. For the salinity, we find increasing volume transport of light waters out of the Labrador Sea to account for 60 % of the freshening, with 27 % due to decreasing northward transport from the Gulf Stream (due to weakening modelled AMOC). The small remainder is a combination of along-track external fluxes and changes in TS properties in the origin regions.

For temperature, the picture is more complicated, half of the overall mean cooling of the water leaving the combined origin regions is mitigated along-track by reduced heat loss to the atmosphere from the originally cooler water. Hence, while surface salinities in the eastern subpolar North Atlantic have shown extreme freshening (the freshest in 120 years (Holliday et al., 2020)), temperatures, though cooler than average, have shown a relatively smaller decrease. The net cooling of water leaving the combined origin regions is, as for salinity, driven mostly by increasing volumes of water originating from the Labrador Sea (over 55 %) and decreasing volume of water from the Gulf Stream (20 %). In contrast to the freshening, a notable contribution to the cooling is also made by the reduced mean temperature of water from the Gulf Stream at their origin (15 %).

For the mechanisms underpinning changes in the basin-scale overturning (AMOC) in the model, relevant here as the reducing modelled transport from the Gulf Stream northward to the subpolar region, we refer the reader to Biastoch et al. (2021). Hindcasts of the past 50–60 years in this eddy-rich model realistically simulate the large-scale circulation, including the AMOC (Biastoch et al., 2021). In contrast to Bryden et al. (2020) who, using heat and freshwater budgets, find that reduced northwards

https://doi.org/10.5194/os-2022-18
Preprint. Discussion started: 11 April 2022

fluxes from the subtropics to the subpolar North Atlantic can explain the majority of the eastern subpolar North Atlantic cooling and freshening, we find these processes to make a minor contribution compared to subpolar gyre-scale processes.

Exploring the subpolar gyre-scale mechanisms driving the exceptional freshening and cooling, with particular reference to the published mechanisms – subpolar gyre strengthening and/or expansion (see e.g. Bersch, 2002; Sarafanov, 2009; Bersch et al., 2007; Hátún et al., 2005; Koul et al., 2020) and the rearrangement of heat and freshwater in the upper subpolar gyre caused by changing pathways of LC-Arctic water (Holliday et al., 2020) – we find neither of these to be fully convincing. Instead, tracking particles further upstream and using detailed analysis of water mass transformations, we find increased volumes of lighter water transported out of the Labrador Sea to be due to deepening isopycnals, in turn due to reduced surface heat loss within the Labrador Sea.

We further find the increased volumes transported from the Labrador Sea to the upper 500 m of $\mathrm{OSNAP_E}$ to be primarily LC-Atlantic water recirculating in the subpolar gyre, rather than the closer inshore LC-Arctic outflow explored by Holliday et al. (2020). This increased recirculation, in both absolute volume terms and the proportion of the surface subpolar gyre circulation, implies longer residence times in the upper layers of the subpolar gyre. The implications of this for subpolar and overturning dynamics remain the subject of further work.

It is interesting to contrast these results with those of Robson et al. (2016) who also propose a link between Labrador Sea densities and cooling of the upper eastern subpolar North Atlantic. But, while Robson et al. (2016) link the eastern subpolar North Atlantic cooling to record low densities (lighter water) in the *deep* Labrador Sea (in turn reducing transport of warm water from the south associated with decreased AMOC), here we find the link is to increased volumes of lighter water in the *upper* water column.

While the model results have enabled us to form a hypothesis, describing a possible mechanism linking Labrador Sea surface heat fluxes with salinity and temperature changes in the eastern Subpolar North Atlantic, comparison of the model output with observational data supports this hypothesis. VIKING20X is shown to reproduce not only the detailed spatial structure of the exceptional freshening event seen in EN4 observations (Fig. 1), but also the evolution of the Labrador Sea vertical structure. This model-data comparison (Fig. 14) shows similar isotherm and isopycnal deepening.

Deepening isopycnals in the upper 500–1000 m of the Labrador Sea outflow, and the resulting increased outflow of lighter waters, has been shown here to lead to freshening and cooling of the upper eastern subpolar North Atlantic. The increased layer thickness of surface waters in the outflow must reduce the thickness of intermediate and/or deep outflows below. Both of these deeper layers also export water which is relatively fresh and cool compared to other North Atlantic water masses of similar density. While a full freshwater and heat budget of the subpolar gyre is beyond the scope of the current work, this suggests that the the exceptional freshening and cooling of the upper 500–1000 m of 2012 to 2016 may represent a change in the vertical distribution of heat and freshwater. This contrasts with the largely horizontal redistribution within the subpolar gyre proposed by Holliday et al. (2020), and the south–north redistribution of Bryden et al. (2020). Some support for the vertical redistribution of heat and salt in the subpolar gyre can be seen in the vertical sections of model temperature and salinity anomalies presented here (Fig. 1e,f) and the OSNAP observational sections (Holliday et al., 2018, Fig. 6), which both show warming and salinification below the thermocline.

https://doi.org/10.5194/os-2022-18
Preprint. Discussion started: 11 April 2022

Tracking particles further upstream shows the primary source of the increased volume of lighter water transported out of the Labrador Sea is the increased volume of water of this density class recirculating in the SPG.

While here we investigate a single historically exceptional event, the primary driving mechanisms we discover – reduced Labrador Sea surface heat loss and reduced meridional overturning circulation – suggest this may form part of the longer-term 'warming hole' phenomenon in the subpolar North Atlantic associated with the changing climate. Again, more work and sustained scientific ocean observations are needed to confirm this hypothesis.

Code and data availability. EN.4.2.2 data were obtained from https://www.metoffice.gov.uk/hadobs/en4/ and are © Crown Copyright, Met Office, 2022, provided under a Non-Commercial Government Licence http://www.nationalarchives.gov.uk/doc/non-commercial-government-licence/version/2/. OSNAP data were collected and made freely available by the OSNAP (Overturning in the Subpolar North Atlantic Program) project and all the national programs that contribute to it (www.o-snap.org). The NEMO code is available at https://forge.ipsl.jussieu.fr/nemo/svn/NEMO/releases/release-3.6 (NEMO System Team, 2021). Our experiments are based on revision 6721. OceanParcels Lagrangian tracking code is available at https://oceanparcels.org/, our experiments used v2.2.2. The original underlying VIKING20X model output is available on request from GEOMAR research datamanagement (datamanagement@geomar.de). Python code for running the Lagrangian tracking and analyses and the water mass analysis is available at https://doi.org/10.5281/zenodo.6393655. The trajectory data are available from https://hdl.handle.net/20.500.12085/830c72af-b5ca-44ac-8357-3173392f402b.

Author contributions. ADF and SAC defined the overall research problem. ADF guided the research and methodology and performed the analyses. ADF, CS and WR designed and performed the Lagrangian experiments. NJF contributed analyses of EN4 observations in the Labrador Sea and TM contributed Eulerian analyses of VIKING20X outputs in the NAC. All co-authors discussed and refined the analyses and contributed to the text.

Competing interests. No competing interest are present

Acknowledgements. ADF would like to acknowledge useful discussions with Stefan F. Gary in the early stages of this work. The ocean model simulation was performed at the North German Supercomputing Alliance (HLRN) and on the Earth System Modelling Project (ESM) partition of the supercomputer JUWELS at the Jülich Supercomputing Centre (JSC). We thank the NEMO system team for support. The trajectory simulations were conducted at the Christian-Albrechts-Universität zu Kiel (NESH).

Financial support. We acknowledge funding from the U.K. Natural Environment Research Council (NERC) National Capability programs CLASS (NE/R015953/1), ACSIS (NE/N018044/1), and NERC grants U.K. OSNAP Decade (NE/T00858X/1, NE/T00858X/2, NE/T008938/1) and SNAP-DRAGON (NE/T013400/1, NE/T013494/1). Additional support was received from the European Union Horizon 2020 research

https://doi.org/10.5194/os-2022-18
Preprint. Discussion started: 11 April 2022

and innovation program under grants 727852 (Blue-Action), 818123 (iAtlantic). This output reflects only the author's view and the European Union cannot be held responsible for any use that may be made of the information contained therein. We also acknowledge support from the German Federal Ministry of Education and Research (grant no. SPACES-CASISAC (03F0796A)).

https://doi.org/10.5194/os-2022-18
Preprint. Discussion started: 11 April 2022

References

Barnier, B., Madec, G., Penduff, T., Molines, J. M., Treguier, A. M., Le Sommer, J., Beckmann, A., Biastoch, A., Böning, C., Dengg, J., Derval, C., Durand, E., Gulev, S., Remy, E., Talandier, C., Theetten, S., Maltrud, M., McClean, J., and De Cuevas, B.: Impact of partial steps and momentum advection schemes in a global ocean circulation model at eddy-permitting resolution, Ocean Dynamics, 56, 543–567, https://doi.org/10.1007/s10236-006-0082-1, 2006.

Bersch, M.: North Atlantic Oscillation–induced changes of the upper layer circulation in the northern North Atlantic Ocean, Journal of Geophysical Research, 107, 20–1, https://doi.org/10.1029/2001jc000901, 2002.

Bersch, M., Yashayaev, I., and Koltermann, K. P.: Recent changes of the thermohaline circulation in the subpolar North Atlantic, Ocean Dynamics, 57, 223–235, https://doi.org/10.1007/s10236-007-0104-7, 2007.

Biastoch, A., Schwarzkopf, F. U., Getzlaff, K., Rühs, S., Martin, T., Scheinert, M., Schulzki, T., Handmann, P., Hummels, R., and Böning, C. W.: Regional imprints of changes in the Atlantic Meridional Overturning Circulation in the eddy-rich ocean model VIKING20X, Ocean Science, 17, 1177–1211, https://doi.org/10.5194/os-17-1177-2021, 2021.

Böning, C. W., Behrens, E., Biastoch, A., Getzlaff, K., and Bamber, J. L.: Emerging impact of Greenland meltwater on deepwater formation in the North Atlantic Ocean, Nature Geoscience, 9, 523–527, https://doi.org/10.1038/ngeo2740, 2016.

Bryden, H. L., Johns, W. E., King, B. A., McCarthy, G., McDonagh, E. L., Moat, B. I., and Smeed, D. A.: Reduction in ocean heat transport at 26°N since 2008 cools the eastern subpolar gyre of the North Atlantic Ocean, Journal of Climate, 33, 1677–1689, https://doi.org/10.1175/JCLI-D-19-0323.1, 2020.

Burkholder, K. C. and Lozier, M. S.: Tracing the pathways of the upper limb of the North Atlantic Meridional Overturning Circulation, Geophysical Research Letters, 41, 4254–4260, https://doi.org/10.1002/2014GL060226, 2014.

Chafik, L., Nilsen, J. E. Ø., Dangendorf, S., Reverdin, G., and Frederikse, T.: North Atlantic Ocean Circulation and Decadal Sea Level Change During the Altimetry Era, Scientific Reports 2019 9:1, 9, 1–9, https://doi.org/10.1038/s41598-018-37603-6, 2019.

Cunningham, S. A., Kanzow, T., Rayner, D., Baringer, M. O., Johns, W. E., Marotzke, J., Longworth, H. R., Grant, E. M., Hirschi, J. J., Beal, L. M., Meinen, C. S., and Bryden, H. L.: Temporal variability of the Atlantic meridional overturning circulation at 26.5°N, Science, 317, 935–938, https://doi.org/10.1126/SCIENCE.1141304/SUPPL_FILE/CUNNINGHAM.SOM.PDF, 2007.

Delandmeter, P. and Van Sebille, E.: The Parcels v2.0 Lagrangian framework: New field interpolation schemes, Geoscientific Model Development, 12, 3571–3584, https://doi.org/10.5194/gmd-12-3571-2019, 2019.

Desbruyères, D., Mercier, H., and Thierry, V.: On the mechanisms behind decadal heat content changes in the eastern subpolar gyre, Progress in Oceanography, 132, 262–272, https://doi.org/10.1016/j.pocean.2014.02.005, 2015.

Desbruyères, D., Chafik, L., and Maze, G.: A shift in the ocean circulation has warmed the subpolar North Atlantic Ocean since 2016, Communications Earth & Environment, 2, 1–9, https://doi.org/10.1038/s43247-021-00120-y, 2021.

Fichefet, T. and Maqueda, M. A.: Sensitivity of a global sea ice model to the treatment of ice thermodynamics and dynamics, Journal of Geophysical Research: Oceans, 102, 12 609–12 646, https://doi.org/10.1029/97JC00480, 1997.

Florindo-López, C., Bacon, S., Aksenov, Y., Chafik, L., Colbourne, E., and Penny Holliday, N.: Arctic Ocean and Hudson Bay Freshwater Exports: New Estimates from Seven Decades of Hydrographic Surveys on the Labrador Shelf, Journal of Climate, 33, 8849–8868, https://doi.org/10.1175/JCLI-D-19-0083.1, 2020.

Foukal, N. P. and Lozier, M. S.: Examining the Origins of Ocean Heat Content Variability in the Eastern North Atlantic Subpolar Gyre, Geophysical Research Letters, 45, 275–11, https://doi.org/10.1029/2018GL079122, 2018.

https://doi.org/10.5194/os-2022-18
Preprint. Discussion started: 11 April 2022

Foukal, N. P., Gelderloos, R., and Pickart, R. S.: A continuous pathway for fresh water along the East Greenland shelf, Science Advances, 6, https://doi.org/10.1126/SCIADV.ABC4254/SUPPL_FILE/ABC4254_SM.PDF, 2020.

Fox, A. D. and Haines, K.: Interpretation of water mass transformations diagnosed from data assimilation, Journal of Physical Oceanography, 33, 485–498, https://doi.org/10.1175/1520-0485(2003)033<0485:IOWMTD>2.0.CO;2, 2003.

Fraser, N. J. and Cunningham, S. A.: 120 Years of AMOC Variability Reconstructed From Observations Using the Bernoulli Inverse, Geophysical Research Letters, 48, e2021GL093 893, https://doi.org/10.1029/2021GL093893, 2021.

Good, S. A., Martin, M. J., and Rayner, N. A.: EN4: Quality controlled ocean temperature and salinity profiles and monthly objective analyses with uncertainty estimates, Journal of Geophysical Research: Oceans, 118, 6704–6716, https://doi.org/10.1002/2013JC009067, 2013.

Goosse, H. and Fichefet, T.: Importance of ice-ocean interactions for the global ocean circulation: A model study, Journal of Geophysical Research: Oceans, 104, 23 337–23 355, https://doi.org/10.1029/1999jc900215, 1999.

Gouretski, V. and Cheng, L.: Correction for Systematic Errors in the Global Dataset of Temperature Profiles from Mechanical Bathythermographs, Journal of Atmospheric and Oceanic Technology, 37, 841–855, https://doi.org/10.1175/JTECH-D-19-0205.1, 2020.

Gouretski, V. and Reseghetti, F.: On depth and temperature biases in bathythermograph data: Development of a new correction scheme based on analysis of a global ocean database, Deep Sea Research Part I: Oceanographic Research Papers, 57, 812–833, https://doi.org/10.1016/J.DSR.2010.03.011, 2010.

Griffies, S. M., Biastoch, A., Böning, C., Bryan, F., Danabasoglu, G., Chassignet, E. P., England, M. H., Gerdes, R., Haak, H., Hallberg, R. W., Hazeleger, W., Jungclaus, J., Large, W. G., Madec, G., Pirani, A., Samuels, B. L., Scheinert, M., Gupta, A. S., Severijns, C. A., Simmons, H. L., Treguier, A. M., Winton, M., Yeager, S., and Yin, J.: Coordinated Ocean-ice Reference Experiments (COREs), Ocean Modelling, 26, 1–46, https://doi.org/10.1016/j.ocemod.2008.08.007, 2009.

Häkkinen, S., Rhines, P. B., and Worthen, D. L.: Warm and saline events embedded in the meridional circulation of the northern North Atlantic, Journal of Geophysical Research: Oceans, 116, 3006, https://doi.org/10.1029/2010JC006275, 2011.

Hátún, H., Sande, A. B., Drange, H., Hansen, B., and Valdimarsson, H.: Ocean science: Influence of the atlantic subpolar gyre on the thermohaline circulation, Science, 309, 1841–1844, https://doi.org/10.1126/science.1114777, 2005.

Holliday, N. P., Bacon, S., Cunningham, S. A., Gary, S. F., Karstensen, J., King, B. A., Li, F., and Mcdonagh, E. L.: Subpolar North Atlantic overturning and gyre-scale circulation in the summers of 2014 and 2016, Journal of Geophysical Research: Oceans, 123, 4538–4559, https://doi.org/10.1029/2018JC013841, 2018.

Holliday, N. P., Bersch, M., Berx, B., Chafik, L., Cunningham, S., Florindo-López, C., Hátún, H., Johns, W., Josey, S. A., Larsen, K. M. H., Mulet, S., Oltmanns, M., Reverdin, G., Rossby, T., Thierry, V., Valdimarsson, H., and Yashayaev, I.: Ocean circulation causes the largest freshening event for 120 years in eastern subpolar North Atlantic, Nature Communications, 11, 585, https://doi.org/10.1038/s41467-020-14474-y, 2020.

IPCC: Climate Change 2021: The Physical Science Basis. Contribution of Working Group I to the Sixth Assessment Report of the Intergovernmental Panel on Climate Change, In Press, Cambridge University Press, https://www.ipcc.ch/report/ar6/wg1/, 2021.

Johnson, H. L., Cessi, P., Marshall, D. P., Schloesser, F., and Spall, M. A.: Recent Contributions of Theory to Our Understanding of the Atlantic Meridional Overturning Circulation, Journal of Geophysical Research: Oceans, 124, 5376–5399, https://doi.org/10.1029/2019JC015330, 2019.

Josey, S. A., Hirschi, J. J., Sinha, B., Duchez, A., Grist, J. P., and Marsh, R.: The recent atlantic cold anomaly: Causes, consequences, and related phenomena, Annual Review of Marine Science, 10, 475–501, https://doi.org/10.1146/annurev-marine-121916-063102, 2018.

https://doi.org/10.5194/os-2022-18
Preprint. Discussion started: 11 April 2022

Keil, P., Mauritsen, T., Jungclaus, J., Hedemann, C., Olonscheck, D., and Ghosh, R.: Multiple drivers of the North Atlantic warming hole, Nature Climate Change 2020 10:7, 10, 667–671, https://doi.org/10.1038/s41558-020-0819-8, 2020.

Koul, V., Tesdal, J. E., Bersch, M., Hátún, H., Brune, S., Borchert, L., Haak, H., Schrum, C., and Baehr, J.: Unraveling the choice of the north Atlantic subpolar gyre index, Scientific Reports, 10, 1–12, https://doi.org/10.1038/s41598-020-57790-5, 2020.

Lange, M. and Sebille, E. V.: Parcels v0.9: Prototyping a Lagrangian ocean analysis framework for the petascale age, Geoscientific Model Development, 10, 4175–4186, https://doi.org/10.5194/gmd-10-4175-2017, 2017.

Large, W. G. and Yeager, S. G.: The global climatology of an interannually varying air - Sea flux data set, Climate Dynamics, 33, 341–364, https://doi.org/10.1007/s00382-008-0441-3, 2009.

Li, F., Lozier, M. S., Bacon, S., Bower, A. S., Cunningham, S. A., de Jong, M. F., DeYoung, B., Fraser, N., Fried, N., Han, G., Holliday, N. P., Holte, J., Houpert, L., Inall, M. E., Johns, W. E., Jones, S., Johnson, C., Karstensen, J., Le Bras, I. A., Lherminier, P., Lin, X., Mercier, H., Oltmanns, M., Pacini, A., Petit, T., Pickart, R. S., Rayner, D., Straneo, F., Thierry, V., Visbeck, M., Yashayaev, I., and Zhou, C.: Subpolar North Atlantic western boundary density anomalies and the Meridional Overturning Circulation, Nature Communications, 12, 3002, https://doi.org/10.1038/s41467-021-23350-2, 2021.

Lozier, M. S., Li, F., Bacon, S., Bahr, F., Bower, A. S., Cunningham, S. A., de Jong, M. F., de Steur, L., DeYoung, B., Fischer, J., Gary, S. F., Greenan, B. J. W., Holliday, N. P., Houk, A., Houpert, L., Inall, M. E., Johns, W. E., Johnson, H. L., Johnson, C., Karstensen, J., Koman, G., Le Bras, I. A., Lin, X., Mackay, N., Marshall, D. P., Mercier, H., Oltmanns, M., Pickart, R. S., Ramsey, A. L., Rayner, D., Straneo, F., Thierry, V., Torres, D. J., Williams, R. G., Wilson, C., Yang, J., Yashayaev, I., and Zhao, J.: A sea change in our view of overturning in the subpolar North Atlantic, Science, 363, 516+, https://doi.org/10.1126/science.aau6592, 2019.

Madec, G., Bourdallé-Badie, R., Bouttier, P.-A., Bricaud, C., Bruciaferri, D., Calvert, D., Chanut, J., Clementi, E., Coward, A., Delrosso, D., Ethé, C., Flavoni, S., Graham, T., Harle, J., Iovino, D., Lea, D., Lévy, C., Lovato, T., Martin, N., Masson, S., Mocavero, S., Paul, J., Rousset, C., Storkey, D., Storto, A., and Vancoppenolle, M.: NEMO ocean engine (Version v3.6), Notes du Pôle de modélisation de l'Institut Pierre-Simon Laplace (IPSL), 27, https://doi.org/10.5281/ZENODO.1472492, 2017.

New, A. L., Smeed, D. A., Czaja, A., Blaker, A. T., Mecking, J. V., Mathews, J. P., and Sanchez-Franks, A.: Labrador Slope Water connects the subarctic with the Gulf Stream, Environmental Research Letters, 16, 084 019, https://doi.org/10.1088/1748-9326/AC1293, 2021.

Nurser, A. J., Marsh, R., and Williams, R. G.: Diagnosing water mass formation from air-sea fluxes and surface mixing, Journal of Physical Oceanography, 29, 1468–1487, https://doi.org/10.1175/1520-0485(1999)029<1468:DWMFFA>2.0.CO;2, 1999.

Peterson, B. J., McClelland, J., Curry, R., Holmes, R. M., Walsh, J. E., and Aagaard, K.: Trajectory shifts in the arctic and subarctic freshwater cycle, Science, 313, 1061–1066, https://doi.org/10.1126/science.1122593, 2006.

Robson, J., Ortega, P., and Sutton, R.: A reversal of climatic trends in the North Atlantic since 2005, Nature Geoscience 2016 9:7, 9, 513–517, https://doi.org/10.1038/ngeo2727, 2016.

Rühs, S., Oliver, E. C., Biastoch, A., Böning, C. W., Dowd, M., Getzlaff, K., Martin, T., and Myers, P. G.: Changing Spatial Patterns of Deep Convection in the Subpolar North Atlantic, Journal of Geophysical Research: Oceans, 126, e2021JC017 245, https://doi.org/10.1029/2021JC017245, 2021.

Sanchez-Franks, A., Hameed, S., and Wilson, R. E.: The Icelandic Low as a Predictor of the Gulf Stream North Wall Position, Journal of Physical Oceanography, 46, 817–826, https://doi.org/10.1175/JPO-D-14-0244.1, 2016.

Sarafanov, A.: On the effect of the north Atlantic oscillation on temperature and salinity of the subpolar north Atlantic intermediate and deep waters, ICES Journal of Marine Science, 66, 1448–1454, https://doi.org/10.1093/icesjms/fsp094, 2009.

https://doi.org/10.5194/os-2022-18
Preprint. Discussion started: 11 April 2022

Schmidt, C., Schwarzkopf, F. U., Rühs, S., and Biastoch, A.: Characteristics and robustness of Agulhas leakage estimates: An intercomparison study of Lagrangian methods, Ocean Science, 17, 1067–1080, https://doi.org/10.5194/os-17-1067-2021, 2021.

Speer, K. and Tziperman, E.: Rates of Water Mass Formation in the North Atlantic Ocean, Journal of Physical Oceanography, 22, 93–104, https://doi.org/10.1175/1520-0485(1992)022<0093:rowmfi>2.0.co;2, 1992.

Thyng, K. M., Greene, C. A., Hetland, R. D., Zimmerle, H. M., and DiMarco, S. F.: True colors of oceanography: Guidelines for effective and accurate colormap selection, Oceanography, 29, 9–13, https://doi.org/10.5670/OCEANOG.2016.66, 2016.

Tsujino, H., Urakawa, S., Nakano, H., Small, R. J., Kim, W. M., Yeager, S. G., Danabasoglu, G., Suzuki, T., Bamber, J. L., Bentsen, M., Böning, C. W., Bozec, A., Chassignet, E. P., Curchitser, E., Boeira Dias, F., Durack, P. J., Griffies, S. M., Harada, Y., Ilicak, M., Josey, S. A., Kobayashi, C., Kobayashi, S., Komuro, Y., Large, W. G., Le Sommer, J., Marsland, S. J., Masina, S., Scheinert, M., Tomita, H., Valdivieso, M., and Yamazaki, D.: JRA-55 based surface dataset for driving ocean–sea-ice models (JRA55-do), Ocean Modelling, 130, 79–139, https://doi.org/10.1016/j.ocemod.2018.07.002, 2018.

Tziperman, E.: On the role of interior mixing and air-sea fluxes in determining the stratification and circulation of the oceans, Journal of Physical Oceanography, 16, 680–693, https://doi.org/10.1175/1520-0485(1986)016<0680:OTROIM>2.0.CO;2, 1986.

van Sebille, E., Griffies, S. M., Abernathey, R., Adams, T. P., Berloff, P., Biastoch, A., Blanke, B., Chassignet, E. P., Cheng, Y., Cotter, C. J., Deleersnijder, E., Döös, K., Drake, H. F., Drijfhout, S., Gary, S. F., Heemink, A. W., Kjellsson, J., Koszalka, I. M., Lange, M., Lique, C., MacGilchrist, G. A., Marsh, R., Mayorga Adame, C. G., McAdam, R., Nencioli, F., Paris, C. B., Piggott, M. D., Polton, J. A., Rühs, S., Shah, S. H., Thomas, M. D., Wang, J., Wolfram, P. J., Zanna, L., and Zika, J. D.: Lagrangian ocean analysis: Fundamentals and practices, Ocean Modelling, 121, 49–75, https://doi.org/10.1016/j.ocemod.2017.11.008, 2018.

Walin, G.: On the relation between sea-surface heat flow and thermal circulation in the ocean, Tellus, 34, 187–195, https://doi.org/10.1111/j.2153-3490.1982.tb01806.x, 1982.

Waskom, M. L.: seaborn: statistical data visualization, Journal of Open Source Software, 6, 3021, https://doi.org/10.21105/JOSS.03021, 2021.

Yashayaev, I. and Loder, J. W.: Further intensification of deep convection in the Labrador Sea in 2016, Geophysical Research Letters, 44, 1429–1438, https://doi.org/10.1002/2016GL071668, 2017.